THE JOURNAL OF BIOLOGICAL CHEMISTRY VOL. 288, NO. 8, pp. 5426–5442, February 22, 2013

The Sulfur Carrier Protein TusA Has a Pleiotropic Role in *Escherichia coli* That Also Affects Molybdenum Cofactor Biosynthesis*[S]

Received for publication, October 29, 2012, and in revised form, December 23, 2012 Published, JBC Papers in Press, January 1, 2013, DOI 10.1074/jbc.M112.431569

Jan-Ulrik Dahl[‡], Christin Radon[‡], Martin Bühning[‡], Manfred Nimtz[§], Lars I. Leichert[¶], Yann Denis[‖], Cécile Jourlin-Castelli[**], Chantal Iobbi-Nivol[**], Vincent Méjean[**], and Silke Leimkühler[‡1]

*From the [‡]Institute of Biochemistry and Biology, Department of Molecular Enzymology, University of Potsdam, 14476 Potsdam, Germany, the [§]Helmholtz Center for Infection Research, 38124 Braunschweig, Germany, the [¶]Medizinisches Proteom-Center, Redox-Proteomics Group, Ruhr-Universität Bochum, 44780 Bochum, Germany, and the [‖]Plate-forme Transcriptome, Institut de Microbiologie de la Méditerranée (FR3479), CNRS, and **Laboratoire de Chimie Bacterienne (UMR7283), CNRS, Aix-Marseille Université, 31 Chemin Joseph Aiguier, 13402 Marseille Cedex 20, France*

Background: The sulfur carrier protein TusA is involved in sulfur transfer to different biomolecules in the cell.
Results: TusA is involved in sulfur transfer for molybdopterin.
Conclusion: Direction of sulfur transfer to biomolecules is mediated by the interaction partners of IscS.
Significance: This study furthers the understanding of how sulfur transfer is regulated in bacteria.

The *Escherichia coli* L-cysteine desulfurase IscS mobilizes sulfur from L-cysteine for the synthesis of several biomolecules such as iron-sulfur (FeS) clusters, molybdopterin, thiamin, lipoic acid, biotin, and the thiolation of tRNAs. The sulfur transfer from IscS to various biomolecules is mediated by different interaction partners (*e.g.* TusA for thiomodification of tRNAs, IscU for FeS cluster biogenesis, and ThiI for thiamine biosynthesis/tRNA thiolation), which bind at different sites of IscS. Transcriptomic and proteomic studies of a Δ*tusA* strain showed that the expression of genes of the *moaABCDE* operon coding for proteins involved in molybdenum cofactor biosynthesis is increased under aerobic and anaerobic conditions. Additionally, under anaerobic conditions the expression of genes encoding hydrogenase 3 and several molybdoenzymes such as nitrate reductase were also increased. On the contrary, the activity of all molydoenzymes analyzed was significantly reduced in the Δ*tusA* mutant. Characterization of the Δ*tusA* strain under aerobic conditions showed an overall low molybdopterin content and an accumulation of cyclic pyranopterin monophosphate. Under anaerobic conditions the activity of nitrate reductase was reduced by only 50%, showing that TusA is not essential for molybdenum cofactor biosynthesis. We present a model in which we propose that the direction of sulfur transfer for each sulfur-containing biomolecule is regulated by the availability of the interaction partner of IscS. We propose that in the absence of TusA, more IscS is available for FeS cluster biosynthesis and that the overproduction of FeS clusters leads to a modified expression of several genes.

Sulfur, an important element in all living cells, is incorporated into proteins not only in the form of cysteine and methionine, but also as iron-sulfur (FeS) clusters and sulfur-containing cofactors and vitamins, and into RNA through a variety of modifications (1, 2). Sulfur is delivered to these various biosynthetic pathways by complex processes involving the successive transfer of sulfur as a persulfide between multiple proteins. In *Escherichia coli*, the iron-sulfur cluster (ISC)[2] system fulfills a housekeeping function (3). The initial sulfur mobilization step is catalyzed by IscS forming a protein-bound persulfide after the conversion of L-cysteine to L-alanine (4). IscS delivers the sulfur to several sulfur-accepting proteins such as IscU, TusA, and ThiI and, as shown recently, to rhodanese-like proteins such as YnjE (5, 6), thereby providing sulfur for different metabolic pathways like the assembly of FeS cluster, thiamine, biotin, and lipoic acid, tRNA modification, or molybdenum cofactor (Moco) biosynthesis. Recent studies by Shi *et al.* (7) map the different binding sites for proteins that interact with IscS. Although the ISC operon encodes the major FeS assembly pathway, a second system exists in *E. coli*, which is encoded by the *sufABCDSE* operon and contains components of a secondary pathway of iron-sulfur cluster assembly; this system is required mainly for the synthesis of FeS clusters under oxidative stress and iron starvation (8).

The TusA protein functions as a sulfur mediator for the synthesis of 2-thiouridine of the modified wobble base 5-methylaminomethyl-2-thiouridine $(mnm)^5s^2U$ in tRNA (9). It interacts with IscS and stimulates its L-cysteine desulfurase activity

* This work was supported by Deutsche Forschungsgemeinschaft Grant LE1171/5-3 (to S. L.).The exchange of researchers among the laboratories involved in the work was funded by the DAAD (German Academic Exchange Program)-PROCOPE program (to C. I.-N. and S. L.).
[S] This article contains supplemental Tables S1–S3.
[1] To whom correspondence should be addressed. Tel.: 49-331-977-5603; Fax: 49-331-977-5128; E-mail: sleim@uni-potsdam.de.

[2] The abbreviations used are: ISC, iron-sulfur cluster; mnm, methylaminomethyl; Moco, molybdenum cofactor; MPT, molybdopterin; MGD, molybdopterin guanine dinucleotide; MCD, molybdopterin cytosine dinucleotide; cPMP, cyclic pyranopterin monophosphate; ICP-OES, inductively coupled plasma optical emission spectrometry; IPTG, isopropyl β-D-thiogalactopyranoside; NR, nitrate reductase; SPR, surface plasmon resonance; TMAO, trimethylamine *N*-oxide; TMAOR, trimethylamine *N*-oxide reductase; AEBSF, 4-(2-aminoethyl)-benzensulfonylfluoride; DMSO, dimethyl sulfoxide; *Ec*, *E. coli*; *Rc*, *R. capsulatus*; hSO, human sulfite oxidase; XDH, xanthine dehydrogenase.

3-fold (9). The persulfide sulfur on TusA-Cys-19 is then transferred to TusD in the TusBCD complex. TusE likely accepts the sulfur from TusD and then interacts with the MnmA-tRNA complex, in which MnmA catalyzes 2-thiouridine formation at position 34 of the tRNA in an ATP-dependent manner by using the persulfide sulfur of TusE. In total, little is known about the function of the modification of 2-thiouridine. It is proposed that in *E. coli* thiomodified $tRNA^{Lys}$ confers efficient ribosome binding (10, 11) and 2-thio-modified $tRNA^{Glu}$ is required for specific recognition by glutaminyl-tRNA synthetase (12). Thus, the 2-thio-modification of uridine 34 plays a critical role in the decoding mechanism. Recently, Maynard *et al.* (13) identified 2-thiouridine modification of $tRNA^{Lys}$ as additionally responsible for enhanced susceptibility to viral infection by inhibition of programmed ribosomal frameshifting.

Despite its role as a sulfur transfer protein for 2-thiouridine formation, a fundamental role for TusA in the general physiology of *E. coli* was discovered by analyzing a strain deficient in *tusA* (14). High salt concentrations were determined to be crucial for the normal growth of a *tusA*-deficient strain. Later, Ishii *et al.* (15) showed that the FtsZ-ring formation appears to be severely impaired in *tusA*-deficient *E. coli* cells, resulting in the formation of a non-divided filamentous cell.

Because of its pleiotropic effect, we were interested in studying the role of *tusA* in Moco biosynthesis (16). In *E. coli* Moco biosynthesis is divided into four steps: 1) conversion of GTP into cyclic pyranopterin monophosphate (cPMP); 2) insertion of two sulfur atoms into cPMP, forming molybdopterin (MPT); 3) insertion of molybdenum to form Moco; and 4) additional modification of Moco by the covalent addition of GMP or CMP to the C4′-phosphate of MPT, forming either the MPT guanine dinucleotide (MGD) cofactor or the MPT cytosine dinucleotide (MCD) cofactor (17, 18). Two MGD moieties are ligated to the molybdenum atom and form the bis-MGD cofactor (19), which is characteristic for the majority of molybdoenzymes in *E. coli*, such as nitrate reductase. Enzymes of the xanthine oxidase family in *E. coli*, like the aldehyde oxidoreductase PaoABC, contain the MCD cofactor.

In the formation of cPMP from GTP, MoaA and MoaC are involved, with MoaA belonging to the class of *S*-adenosylmethionine-dependent enzymes, which contain a conserved 4Fe4S cluster binding site at the N terminus. MoaA, in addition, contains a C-terminal 4Fe4S cluster, which is unique to MoaA proteins. Further, for the formation of MPT from cPMP, two sulfur atoms are incorporated into the C1′ and C2′ positions of cPMP, a reaction catalyzed by MPT synthase (20). The *E. coli* MPT synthase is a heterotetrameric enzyme consisting of two MoaE and two MoaD subunits (20, 21). In its active form, MoaD contains a C-terminal thiocarboxylate group that acts as a direct sulfur donor for the synthesis of the dithiolene group of Moco (20, 22, 23). For the synthase to act catalytically, it is necessary to regenerate its transferable sulfur, a reaction for which the MoeB protein and ATP is required (20). It has been shown that MoeB solely activates the C terminus of MoaD by the formation of an acyl-adenylate, and the L-cysteine desulfurase IscS in its persulfide-bound form has been identified as the primary physiological sulfur-donating enzyme for the generation of thiocarboxylate on MPT synthase (24, 25). Recently, it has been shown that the rhodanese-like protein YnjE works in conjunction with IscS to make the sulfur transfer to MoaD more specific (5).

Here, we report that a disruption in the *tusA* gene has a pleiotropic effect on the transcription of genes in *E. coli*. Microarray analyses showed that the transcription of several genes involved in Moco biosynthesis and FeS cluster biosynthesis, and additionally of genes encoding for hydrogenase and several molybdoenzymes, was increased. Surprisingly, the activity of several molybdoenzymes in the Δ*tusA* strain was drastically decreased. Further analyses showed that TusA has an effect on the direction of sulfur transfer of IscS to the various sulfur-accepting biomolecules. In the absence of TusA, sulfur transfer to FeS clusters is increased, thereby effecting the expression of several genes in *E. coli*. Here we present a model explaining the different effects of TusA under various growth conditions in *E. coli* with a focus on Moco biosynthesis.

EXPERIMENTAL PROCEDURES

Bacterial Strains, Plasmids, Media, and Growth Conditions—The strains and plasmids used in this study are listed in Table 1. All isogenic BW25113 mutant strains used for various assays were obtained from the Keio collection (26). Verification of the mutant strains was performed either by PCR amplification or by functional complementation studies of the respective genes. If necessary, DE3 lysogens of *E. coli* strains were generated by using the DE3 lysogenization kit (Novagen) following the manufacturer's instructions. Bacterial cultures were generally grown in LB medium, and when required, 150 μg/ml ampicillin, 25 μg/ml kanamycin, or 50 μg/ml chloramphenicol was added to the medium.

RNA Isolation for Microarray Analysis—Experiments were performed with *E. coli* strains BW25113 and JW3435 (Δ*tusA*) grown both aerobically and anaerobically and supplemented with 20 mM nitrate as electron acceptor to mid-log phase. Total RNA was isolated with the High Pure RNA Isolation Kit (Roche Applied Biosystems) with two DNase I treatments. RNA concentration was determined by its absorbance at 260 nm. DNA contaminations were checked by PCR on each RNA sample. The quality of RNA was analyzed by using a Bioanalyzer (Agilent Technologies).

Global Transcriptional Analysis—The ChipShot™ labeling clean-up system (Promega) was used to generate fluorescent labeled cDNA via direct incorporation of Cy®3- and Cy®5-labeled nucleotides (GE Healthcare). The reverse transcription reaction was performed in the presence of 10 μg of total RNA and random hexamers according to the manufacturer's recommendations. Two independent cDNA preparations were labeled once with each dye (reverse dye labeling) to account for sampling differences, biases in dye coupling or emission efficiency of Cy® dyes. Labeled cDNA was purified from contaminating fluorescent dNTPs and degraded RNA using the ChipShot labeling clean-up system (Promega). Dye incorporation efficiency was determined by absorbance readings at 260, 550, and 650 nm, and the frequency of incorporation (pmol of dye incorporated/ng of cDNA) was calculated according to Promega's instructions. Optimally labeled samples were combined, vacuum-dried, and resuspended to a final volume of 50 μl in GE

TABLE 1
***E. coli* strains and plasmids used in this study**

Plasmid or strain	Genotype or relevant characteristics	Source or reference
Plasmids		
pJD8	Gene region − 198 bp to − 1 bp upstream of *ydjXYZynjABCD* transcriptional start cloned into EcoRI/BamHI sites of pGE593, Amp^R	This study
pJD14	Gene region − 208 bp to − 1 bp upstream of *ynjE* transcriptional start cloned into EcoRI/BamHI sites of pGE593, Amp^R	This study
pJD27	Gene region − 201 bp to − 1 bp upstream of *tusA* transcriptional start cloned into *Eco*RI/*Bam*HI sites of pGE593, Amp^R	This study
pJD28	Gene region − 187 bp to − 1 bp upstream of *tusD* transcriptional start cloned into EcoRI/BamHI sites of pGE593, Amp^R	This study
pJD66	Gene region − 200 bp to − 1 bp upstream of *iscRSUA* transcriptional start cloned into EcoRI/BamHI sites of pGE593, Amp^R	This study
pJD84	Gene region − 200 bp to − 1 bp upstream of *pepT* transcriptional start cloned into *Eco*RI/*Bam*HI sites of pGE593, Amp^R	This study
pJD34	*tusA* gene cloned into NdeI and BamHI sites of pET11b, Amp^R	This study
pJD35	*tusA* gene cloned into NdeI and BamHI/BglII sites of pACYCDuet, Cm^R	This study
pJD49	*tusAC19S* gene cloned into NdeI and BamHI sites of pET11b, Amp^R	This study
pJD54	*iscU* gene cloned into NdeI and BamHI sites of pET28a, Km^R	This study
pGE593	pBR322Δ*tet lacZ lacY'*	(50)
pET11b	T7-RNA polymerase-based expression vector, Amp^R	Novagen
pET28a	T7-RNA polymerase-based expression vector, km^R	Novagen
pET15b	T7-RNA polymerase-based expression vector, Amp^R	Novagen
pACYCDuet	T7-RNA polymerase-based expression vector, Cm^R	Novagen
pMW15eBaDaE	*moaDEmoeB* genes cloned into NcoI and BamHI sites of pET15b, Amp^R	(23)
pDB1282	*iscSUAhscABfdxiscX* genes cloned into NcoI site of pAra13, Amp^R	51
pJF119	Expression vector with pBR replication origin, Amp^R	(52)
pTrcHis	Expression vector pTrcdel containing the His_6-Tag and *trc* promotor, Amp^R	(34)
pMN100	*paoABC* genes cloned into NdeI and SacI sites of pTrcHis, Amp^R	33
pTG718	Genes encoding for human sulfite oxidase cloned into pTrcHis, Amp^R	(34)
pTorAD	*torAD* genes cloned into pJF119, Amp^R	(32)
pSL207	*xdhABC* genes cloned into NdeI and HindIII sites of pTrcHis, Amp^R	(35)
Strains		
BW25113	*laclq rrnBT14* Δ*lacZWJ16 hsdR514* Δ*araBADAH33* Δ*rhaBADLD78*	(26)
JW3435 (Δ*tusA*)	*BW25113*Δ*tusA*:::*km*	(26)
JW3307 (Δ*tusD*)	*BW25113*Δ*tusD*:::*km*	(26)
JW1119 (Δ*mnmA*)	*BW25113*Δ*mnmA*:::*km*	(26)
JW0764 (Δ*moaA*)	*BW25113*Δ*moaA*:::*km*	26
JW0767 (Δ*moaD*)	*BW25113*Δ*moaD*:::*km*	(26)
JW1994 (Δ*yeeD*)	*BW25113*Δ*yedF*:::*km*	(26)
JW1915 (Δ*yedF*)	*BW25113*Δ*yeeD*:::*km*	(26)
JW3435/1994/1915 (Δ*tusA*Δ*yeeD*Δ*yedF*)	*BW25113*Δ*yeeD*Δ*yedF*Δ*tusA*:::*km*	This study
MC4100	*F⁻ [araD139]B/r* Δ*(argF-lac)169* λ- e14- flhD5301* Δ*(fruK-yeiR)725 (fruA25)≠ relA1 rpsL150(strR) rbsR22* Δ*(fimB-fimE)632(::IS1)*	(53)
IMW151a	*MC4100* Δ*fnr*::*tet*	(54)

hybridization buffer (HI-RPM). The combined target cDNA samples were hybridized to the spotted slides for 17 h at 65 °C in an Agilent hybridization chamber. Following hybridization, slides were washed in Agilent wash buffers as recommended by the manufacturer and dried.

Agilent microarrays (*E. coli* gene expression microarray, 8 × 15 K (clustering), G4813A-020097, Agilent) were then scanned with an Axon Genepix 4400A (MDS Analytical Technologies) at a resolution of 5 μm/pixel. Scans stored as 16-bit TIFF (tagged information file format) image files and data analysis were performed with GenePix Pro 7.2. Low quality spots (spots smaller than 40 μm in diameter and/or exhibiting a signal-noise ratio higher than 2) were flagged and filtered out. Median values for each spot were log transformed (log_2) and normalized by the Lowess method to account for any difference in total intensity between the scanned images using Acuity microarray analysis software (version 4.0; Axon Instrument Inc.). Two independent microarray experiments were performed. A 1.0-fold difference from the 1:1 hybridization ratio was taken as indicative of differential gene expression.

Two-dimensional Gel Electrophoresis—50-ml cultures of strains BW25113 and JW3435 (Δ*tusA*) were grown aerobically at 37 °C for 8 h. Cells were harvested, resuspended in 1 ml of 10 mM Tris-HCl (pH 7.5), and sonified. Cell lysates were centrifuged at 18,000 × *g* for 30 min. The proteins of the supernatants were purified with the 2D Clean-Up Kit (GE Healthcare) from nucleic acids, lipids, and salt and resuspended in a rehydration solution (10% glycerol, 8 M urea, 2% (w/v) CHAPS, 2% (v/v) IPG buffer (pH 4–7 L), 19 mM DTT, and 4 mM AEBSF). Linear immobilized pH 4–7 L gradient strips (13 cm, GE Healthcare) were rehydrated overnight in rehydration solution containing 600 μg of total protein. First dimension isoelectric focusing was performed by using a PROTEAN IEF Cell (Bio-Rad) as follows: 15 min at 150 V, 15 min at 300 V, 10 min at 500 V, 10 min at 1,000 V, 10 min at 1500 V, 10 min at 2000 V, 10 min at 2500 V, and 10 min 3000 V. The last step was performed at 3500 V until 20,000 volt hours were reached. For all steps a linear voltage step was used and the current was limited to 50 μA/gel. After the isoelectric focusing, the IPG strips were re-equilibrated for 15 min in 30% (v/v) glycerol, 50 mM Tris-HCl (pH 8.8), 6 M urea, 2% (w/v) SDS, and 1% (w/v) DTT, washed with water, and additionally incubated for 15 min in 30% (v/v) glycerol, 50 mM Tris-HCl (pH 8.8), 6 M urea, 2% (w/v) SDS, and 2.5% (w/v) iodacetamide. For the second dimension, IPG strips were placed on

12% SDS-polyacrylamide gels (Bio-Rad system, 1-mm spacer) and fixed with agarose. The gels were run for 30 min at 200 V (10 mA/gel) and for 4.5 h at 400 V (20 mA/gel). Gels were stained with colloidal Coomassie Brilliant Blue and destained with water.

MALDI-TOF MS—Peptide mapping was performed on a Bruker ULTRAFLEX time-of-flight (TOF/TOF) instrument in the positive mode using the reflectron for enhanced resolution and a matrix of α-cyano-4-hydroxycinnamic acid. For MS/MS analyses, selected parent ions were subjected to laser-induced dissociation, and the resulting fragment ions were separated by the second TOF stage of the instrument. 1-μl samples at an approximate concentration of 1–10 pmol/μl were mixed with equal amounts of matrix. This mixture was spotted onto a stainless steel target and dried at room temperature before analysis.

*Construction of the E. coli Δ*tusA*Δ*yedF*Δ*yeeD Triple Mutant Strain*—As described previously, the mutation of strain JW1994 (Δ*yeeD*) and JW1915 (Δ*yedF*) was transferred to JW3435 (Δ*tusA*) by P1 transduction (17), resulting in Δ*tusA*Δ*yeeD*Δ*yedF* strain JW3435/1994/1915.

Enzyme Assays—Strains BW25113, JW3435 (Δ*tusA*), JW3307 (Δ*tusD*), JW1119 (Δ*mnmA*), JW0764 (Δ*moaA*), JW1994 (Δ*yeeD*), JW1915 (Δ*yedF*), and JW3435/1994/1915 (Δ*tusA*/Δ*yeeD*/Δ*yedF*) (26) were grown aerobically and anaerobically for 10 h in 15 ml of LB medium at 37 °C in the presence of 20 mM KNO_3 or TMAO. 15 ml of culture was harvested, resuspended in 50 mM Tris-HCl (pH 7.5) for nitrate reductase (NR) activity measurements or in 100 mM potassium-phosphate buffer (pH 6.5) for TMAO reductase (TMAOR) activity measurements, and sonified. Aliquots of 50–200 μl of each extract were analyzed for NR activity in a total volume of 4 ml of an assay mixture containing 0.3 mM benzyl viologen, 10 mM KNO_3, and 20 mM Tris (pH 7.5). For TMAOR activity, the same volumes of cell extract were analyzed in a total volume of 4 ml of an assay mixture containing 0.4 mM benzyl viologen, 5 mM TMAO, and 100 mM potassium-phosphate buffer (pH 6.5). The reaction was initiated by the injection of sodium dithionite into the anaerobic assay mixture. The oxidation of reduced benzyl viologen at 600 nm was measured for 1 min, and the units of activity were calculated as described elsewhere (27). The protein concentration of each extract was determined using the Bradford assay (Pierce). Hydrogenase activity was estimated spectrophotometrically by measuring oxidized benzyl viologen reduction at 600 nm in the presence of H_2-saturated buffer (28).

For the determination of overall L-cysteine desulfurase activity, plasmids pJD35 (encoding TusA), pJD54 (encoding IscU), and pACYCDuet were expressed in BW25113(DE3) in the presence of 20 μM IPTG for 8 h. Cells were harvested, resuspended in 50 mM Tris-HCl, 200 mM NaCl, 10 μM pyridoxal-5-phosphate (PLP), and 2 mM dithiothreitol (pH 8.0), sonified, and centrifuged for 20 min at 18,000 × *g* at 4 °C. The L-cysteine desulfurase activity of the supernatants was measured by determining the total sulfide concentration as described previously (29). Supernatants were incubated with 500 μM L-cysteine in a total volume of 800 μl for 10 min at 30 °C. The reactions were stopped by the addition of 100 μl of 20 mM *N*,*N*-dimethyl-*p*-phenylenediamine in 7.2 M HCl and 100 μl of 30 mM $FeCl_3$ in 1.2 M HCl. After an incubation time of 20 min, the precipitated protein was removed by centrifugation, and methylene blue was measured at 670 nm. A standard curve was generated using known amounts of sodium sulfide as the sulfur source.

Detection of the Total MPT Content—50 ml of LB cultures of strains BW25113, JW3435 (Δ*tusA*), JW1119 (Δ*mnmA*), JW0764 (Δ*moaA*), and JW0767 (Δ*moaD*) were grown aerobically and anaerobically for 8 h in the presence of 20 mM nitrate, harvested by centrifugation, and resuspended in 3 ml of 100 mM Tris-HCl (pH 7.2). The lysate was obtained by sonication. The total MPT content of the strains was determined by form A detection as described previously (5).

Detection of cPMP— cPMP was converted to compound Z purified from *E. coli* cell extracts of the strains BW25113, JW3435 (Δ*tusA*), JW1119 (Δ*mnmA*), JW0764 (Δ*moaA*), and JW0767 (Δ*moaD*). 50 ml of LB cultures of each strain containing 20 mM nitrate were grown aerobically or anaerobically for 8 h, harvested by centrifugation, and resuspended in 3 ml of H_2O. The lysate was obtained by sonication. cPMP was converted to its fluorescent derivative, compound Z, by adjusting the pH of the supernatant to 2.5 with HCl and adding 200 μl of 1% (w/v) I_2, 2% (w/v) KI for 14 h. Excess iodine was removed by the addition of 110 μl of 1% (w/v) ascorbic acid, and the sample was adjusted with 1 M Tris to pH 8.3. Compound Z was further purified on a QAE ion exchange column (Sigma) with a 500-μl bed volume, which was equilibrated in H_2O. Compound Z was eluted from the matrix in a volume of 5 ml (5 × 1 ml fractions). The reactions were analyzed by subsequent injection (100 μl) onto a C18 reversed phase HPLC column (4.6 × 250-mm ODS Hypersil; particle size, 5 μm) equilibrated with 10 mM potassium phosphate (pH 3.0) with 1% methanol at an isocratic flow rate of 1 ml/min. In-line fluorescence was monitored by an Agilent 1100 series detector with excitation at 370 nm and emission at 450 nm. Plasmids pJD34 (encoding TusA) and pJD49 (encoding TusA-C19S) were introduced into Δ*tusA* strain. As a control, pET11b containing Δ*moaD* was used. Cells were cultivated in the presence or absence of 50 μM IPTG. cPMP accumulated in these cells was determined as described above.

Analysis of the Sulfuration Level of MPT Synthase Purified from Different E. coli Mutant Strains—For expression of MPT synthase, the plasmid encoding active MPT synthase (expressing MoaD, MoaE, and MoeB) was introduced into *E. coli* BW25113(DE3), JW3435 (Δ*tusA*) (DE3), and JW1119 (Δ*mnmA*) (DE3) cells, respectively. Expression and purification of *E. coli* MPT synthase were performed following published procedures (23). Protein concentration was determined using the calculated extinction coefficient at 280 nm. MPT synthase reactions were performed at room temperature in a total volume of 400 μl of 100 mM Tris (pH 7.2). The reaction mixtures contained 15 μM overexpressed MPT synthase. The reaction was initiated by the addition of an excess amount of cPMP, which was purified according to published procedures (30). The MPT produced was oxidized to form A and quantified following published procedures (27, 31).

Expression and Purification of EcPaoABC, EcTorAD, hSO, and RcXDH—Plasmids pMN100 (coding for PaoABC), pSL207 (coding for *Rc*XDH), pTorAD (coding for TMAO reductase),

and pTG718 (coding for hSO) were expressed in *E. coli* BW25113 and JW3435 (Δ*tusA*) cells. The enzymes were purified by nickel-nitrilotriacetic acid chromatography following published procedures (32–35). The enzyme activities of the four enzymes were measured spectrophotometrically as described elsewhere (33, 36–38). Moco/MPT was quantified by conversion to form A as described previously (31). Oxidation was performed either at room temperature for 14 h (for hSO and *Rhodobacter capsulatus* XDH) or for 30 min at 95 °C (for *E. coli* TorAD and *E. coli* PaoABC). The molybdenum and iron contents of the purified proteins were quantified by inductively coupled plasma optical emission spectrometry (ICP-OES) analysis with a PerkinElmer Life Sciences Optima 2100 DV ICP-OES. 500 μl of a 10 μM solution was mixed with 500 μl of 65% nitric acid and incubated overnight at 100 °C before the addition of 4 ml of water.

Metal Analysis—For metal analysis of total crude extract (A) and membrane fraction (B), strains BW25113, JW3435 (Δ*tusA*), JW1119 (Δ*mnmA*), and JW0764 (Δ*moaA*) were grown aerobically for 10 h in 100 ml of LB at 37 °C. Cultures were harvested, washed three times with 10 ml of 50 mM Tris-HCl (pH 7.5), resuspended in 3 ml of the same buffer, and sonified. 2 ml of disrupted cells were centrifuged at 18,000 × *g* for 30 min. The membrane fraction was then washed three times with 5 ml of 50 mM Tris-HCl (pH 7.5) and resuspended in 1 ml of the same buffer. The molybdenum, iron, nickel, and copper contents of the *E. coli* strains were quantified in total crude extract and membrane fraction. As a reference, the multi-element standard solution XVI (Merck) was used.

β-*Galactosidase Activity*— *E. coli* strains BW25113, Δ*tusA*, Δ*iscR,* MC4100, and Δ*fnr* carrying *tusA-lacZ* reporter plasmid pJD27, *tusBCD-lacZ* reporter plasmid pJD28, *ydjXYZynjABCD-lacZ* reporter plasmid pJD8, *ynjE-lacZ* reporter plasmid pJD14, iscRSUA-lacZ reporter plasmid pJD66, pepT-lacZ reporter plasmid pJD83, or pGE593 were grown in LB under aerobic or anaerobic conditions. Following growth to $A_{600\,nm}$ 0.6–1.0, β-galactosidase activities were measured by the SDS-chloroform method, and the units of activity were calculated as Miller units for each sample using the equation $MU = 1000 \times [A_{420} - 1.75 \times A_{550}][A_{600} \times t \times V]$, where *t* equals the time of reaction and *V* equals the volume (ml) of cells added to the assay tubes.

Expression of the Genes from the ISC Operon, tusA, and iscU—Plasmids pDB1282 (coding for *Azotobacter vinelandii* IscS, IscU, IscA, HscB, HscA, Fdx, and IscX), pJD34 (coding for TusA), pJD54 (coding for IscU), pET15b, and pEB327 were expressed in the BW25113(DE3) strain. Expression of TusA, IscU, and pET15b was induced by the addition of 20 μM IPTG for 8 h. Expression of both the ISC genes and pEB327 was induced by the addition of 0.1% arabinose. Cells were harvested, and NR and TMAOR activity was measured in the same manner as described above for the mutant strains.

Surface Plasmon Resonance (SPR) Measurements—All binding experiments were performed with the SPR-based instrument Biacore™ T200 on CM5 sensor chips at a temperature of 25 °C and a flow rate of 10 μl/min using Biacore control T200 software and evaluation T200 software (GE Healthcare) as described previously (39). The autosampler racks containing the sample vials were cooled to 4 °C. Immobilization of proteins yielded the following resonance units (RU)/flow cell: BSA, 1204 RU; IscS, 1118 RU; TusA, 538 RU; IscU, 1049 RU. For immobilization, 10 mM acetate buffer with variable pH (pH 4.0 for TusA and IscU and pH 5.0 for IscS) was used.

As a running buffer, 20 mM phosphate, 150 mM NaCl, and 0.005% Tween 20 (pH 7.4) was used. IscS, IscU, and TusA with concentrations of 0.8, 1.6, 3.1, 6.3, 12.5, and 25 μM were injected for 4.5 min at a flow rate of 30 μl/min followed by 15 min of dissociation using the KINJECT command and regeneration of the sensor surface with 50 mM HCl for 1 min. As a control, BSA was used as ligand. Binding curves were corrected by subtracting buffer injection curves for all four flow cells.

RESULTS

Microarray Analysis—In previous studies, TusA was shown to be involved in the modification of tRNA, in cell morphology, in cell division, and in receptivity for viral infection (9, 13–15). Because of its pleiotropic effects we were interested in analyzing the role of TusA further. To reveal an effect of the absence of TusA on gene expression, we chose a microarray approach and compared different growth conditions in *E. coli*. One major effect of TusA influences growth in the exponential ohase as reported previously. Additionally, we wanted to analyze the differences in gene expression in relation to oxygen. *E. coli* BW25113 and Δ*tusA* strains were grown in LB until the stationary phase or mid-exponential phase was reached under aerobic or anaerobic conditions at 37 °C. For expression profiling, samples were taken, total RNA was extracted, converted to Cy®3 and Cy®5-labeled cDNA, and hybridized to *E. coli* DNA microarrays. Microarray analysis showed that deletion of *tusA* led to changes in the regulation of a set of genes of which there is a complete list in supplemental Tables S1–S3. Negative values indicate increased expression in the Δ*tusA* strain, and positive values show higher expression in BW25113 wild type. Among those, we selected some genes of interest encoding for proteins of Moco biosynthesis, molybdoenzymes, hydrogenases, and FeS cluster biosynthesis (Table 2) for further description.

The most pronounced difference in the Δ*tusA* strain grown aerobically to mid-exponential phase was the higher expression of the *moaABCDE* operon, encoding enzymes involved in cPMP/MPT biosynthesis. This effect was the same under the different growth conditions analyzed. The expression of the molybdate transport system (*modABC*) was decreased under aerobic conditions in the stationary phase in the absence of *tusA*. The role of *modF* is thus far unclear. For most molybdoenzymes the expression was increased in the Δ*tusA* strain under anaerobic conditions and under aerobic conditions in the stationary phase. However, in the mid-exponential phase and under aerobic conditions, the expression of genes coding for the molybdoenzymes DMSO reductase, YdhV, YnfE, and NarG was decreased in the Δ*tusA* strain. Additionally, the $\log_2$ ratio of the operon coding for hydrogenase 3 (*hycABCDEFG*) and its maturation factors (*hypA*, *hypN*, and *hypF*) indicated an elevated expression level in the Δ*tusA* strain (Table 2). The expression of the *sufABCDSE* operon was also increased under anaerobic conditions when *tusA* was deleted, whereas it was

TABLE 2

Microarray analysis comparing expression profiles of the Δ*tusA* mutant to BW25113

Gene expression values (log_2 median of ratio) for all genes/operons are differently regulated in Δ*tusA* strain cultivated under different growth conditions. Genes with a log_2 median of ratio larger than ⟨1.0⟩ (corresponding to genes induced more than 2.3-fold) are considered differentially expressed. Negative values indicate higher expression in Δ*tusA* strain; positive values show higher expression in BW25113 wild type. Stat., stationary phase.

Blattner No.	Gene name	Function	Log$_2$ median of ratio (BW25113/Δ*tusA*)		
			O_2	O_2/20 mM KNO_3	O_2
Hydrogenase			*Mid-log*	*Mid-log*	*Stat.*
b2719	*hycG*	Hyd 3 and formate hydrogenase complex		−3.806	
b2720	*hycF*	Formate hydrogenlyase complex FeS protein		−4.278	
b2721	*hycE*	Hyd 3, large subunit		−4.468	
b2722	*hycD*	Hyd 3, membrane subunit		−4.674	
b2723	*hycC*	Hyd 3, membrane subunit		−4.357	
b2724	*hycB*	Hyd 3, FeS cluster subunit		−3.995	
b2725	*hycA*	Formate hydrogenlyase regulatory protein		−4.094	
b2726	*hypA*	Protein for nickel insertion in Hyd 3		−4.046	
b2713	*hydN*	Electron transport protein HydN		−3.012	
b2712	*hypF*	Carbamoyl phosphate phosphatase for maturation		−2.677	
Moco biosynthesis					
b0781	*moaA*	MPT biosynthesis protein A	−3.490	−1.650	−3.576
b0782	*moaB*	MPT biosynthesis protein B	−3.037	−1.582	−3.611
b0783	*moaC*	MPT biosynthesis protein C	−3.050	−1.550	−3.344
b0784	*moaD*	MPT biosynthesis protein D	−3.265	−1.835	−3.460
b0785	*moaE*	MPT biosynthesis protein E	−3.090	−1.834	−3.179
b0763	*modA*	Molybdate transporter subunit			2.855
b0764	*modB*	Molybdate transporter subunit			2.236
b0765	*modC*	Molybdate transporter subunit			1.768
b0760	*modF*	ATP-binding protein		1.109	
Molybdoenzymes					
b0285	*paoB*	PaoABC, FAD-containing subunit			1.352
b0894	*dmsA*	DMSO reductase, anaerobic, subunit A	1.864	1.244	
b0895	*dmsB*	DMSO reductase, anaerobic, subunit B	1.586		
b1222	*narX*	Sensory histidine kinase			−1.176
b1223	*narK*	Nitrate/nitrite transporter	1.463	1.980	−3.095
b1224	*narG*	NR I, α subunit	1.577		−3.834
b1225	*narH*	NR I,β (Fe-S) subunit			−2.076
b1226	*narJ*	Moco assembly chaperone subunit of NR 1			−2.191
b1227	*narI*	NR I, γ (cytochrome b(NR)) subunit			−2.542
b1465	*narV*	NR II, γ subunit		−2.069	
b1466	*narW*	NR II, Δ subunit		−2.321	−1.195
b1467	*narY*	NR II, β subunit		−2.876	−1.323
b1468	*narZ*	NR II, α subunit			−1.490
b1469	*narU*	Nitrate/nitrite transporter		−1.563	
b1476	*fdnI*	Formate dehydrogenase-*N*, Cyt b_{556} subunit		−1.189	
b1587	*ynfE*	Selenate reductase	1.578		2.062
b1673	*ydhV*	Predicted oxidoreductase	1.052		
b2203	*napB*	NR III, Cyt c_{550} subunit			−2.168
b2204	*napH*	Ferredoxin-type protein		1.026	−1.978
b2205	*napG*	Ferredoxin-type protein		1.052	−2.022
b2206	*napA*	NR III, large subunit		1.084	−3.325
b2207	*napD*	Assembly protein for NR III		1.049	−2.133
b2208	*napF*	Ferredoxin-type protein			−3.411
b2469	*narQ*	Sensory histidine kinase		−1.127	
b2881	*xdhD*	XDH homologue		−2.162	
b3892	*fdoI*	Formate dehydrogenase-O, Cyt b_{556} subunit			−1.250
b3893	*fdoH*	Formate dehydrogenase-O, FeS subunit			−1.083
b3894	*fdoG*	Formate dehydrogenase-O, large subunit			−1.457
b4079	*fdhF*	Formate dehydrogenase-H, α subunit		−3.415	
FeS cluster biosynthesis					
b2527	*hscB*	Molecular chaperone for IscU			1.175
b2528	*iscA*	FeS assembly protein			1.114
b1679	*sufE*	Sulfur acceptor protein		−2.190	1.201
b1680	*sufS*	L-cysteine desulfurase	1.410	−2.297	1.666
b1681	*sufD*	FeS assembly protein		−2.750	1.476
b1682	*sufC*	FeS assembly protein	1.320	−2.354	1.762
b1683	*sufB*	FeS assembly protein	1.707	−2.376	1.717
b1684	*sufA*	FeS assembly protein	1.712	−2.352	1.796
2-thiouridine formation					
b1133	*mnmA*	tRNA-specific 2-thiouridylase	−1.069	−1.577	
b3343	*tusB*	2-Thiouridine-synthesizing protein B		1.108	
b3470	*tusA*	2-Thiouridine-synthesizing protein A	2.136	2.576	2.606

decreased under aerobic conditions. The expression of the *iscA* and *hcsB* genes, involved in housekeeping FeS cluster biosynthesis, was also decreased under aerobic conditions in the stationary phase. Genes for tRNA thiolation were also altered, with an increased expression of *mnmA* and a decreased expression of *tusB*.

Two-dimensional Gel Electrophoresis—To confirm the results obtained by microarray analysis of the Δ*tusA* strain, we wanted additionally to check the changes at the protein level of this mutant strain compared with the corresponding wild type. Therefore two-dimensional gel electrophoresis was used as described under "Experimental Procedures." The soluble pro-

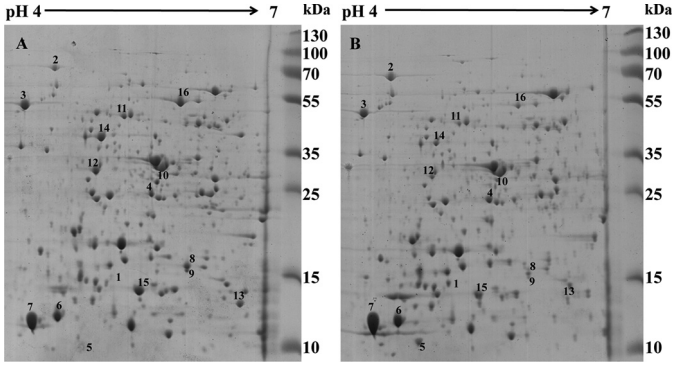

FIGURE 1. **Two-dimensional gel electrophoresis of *E. coli* BW25113 and Δ*tusA* strains.** Soluble cytoplasmic protein fractions were prepared from 50 ml cultures of strains BW25113 (*A*) and JW3435 (Δ*tusA*) (*B*) grown under aerobic conditions for 8 h at 37 °C. 660 μg of total protein was resolved on two-dimensional PAGE. First dimension isoelectric focusing was performed with linear immobilized pH 4–7 gradient strips. For the second dimension 12% SDS-polyacrylamide gels were used. Gels were stained with colloidal Coomassie Brilliant Blue. Molecular mass standards are shown on the *right side* of each gel in kDa. The *numbers* indicate the excised protein spots that were analyzed by MALDI peptide mapping.

tein fractions obtained from strains BW25113 and Δ*tusA* grown aerobically to the beginning of the stationary phase were separated by two-dimensional gel electrophoresis. Fig. 1 shows the colloidal Coomassie-stained two-dimensional gels for BW25113 and the Δ*tusA* strains. The intensity of 16 spots within the gels was identified as different, indicating their different levels of expression. The spots were excised from the gels and analyzed by MALDI peptide mapping. The identified proteins are listed in Table 3, where five proteins were identified in five independent experiments to be expressed differentially in either BW25113 or Δ*tusA*. One of the proteins identified to be present in higher amounts in Δ*tusA* is the MoaE protein (marked with the number *1* in Fig. 1). Expression of peroxyredoxin OsmC and periplasmic dipeptide transport protein DppA was decreased in the Δ*tusA* mutant. In contrast, expression of the chaperone DnaK as well as flagellin FliC was increased in the Δ*tusA* strains (Fig. 1 and Table 3). In comparison with the microarray data, mainly the MoaE protein was identified to be present in higher amounts. Limitations to this two-dimensional gel electrophoresis might explain why the other proteins were not identified in higher amounts. These disadvantages and the small size of, for example, MoaD and MoaC might contribute to the fact that only MoaE was detectable in our proteomic approach.

Transcriptional Analysis of tusA-lacZ and ynjE-lacZ Promotor Fusions in E. coli BW25113 under Aerobic and Anaerobic Conditions—The microarray analysis identified differences in the expression of genes in the Δ*tusA* mutant under aerobic and anaerobic conditions. To study the expression of *tusA* in relation to oxygen, we constructed a *tusA-lacZ* fusion. We analyzed the expression level of *tusA-lacZ* in comparison with a *tusD*-lacZ fusion, the promoter of which controls the genes of the *tusBCD* operon. Additionally, we analyzed the expression of *ynjE*, as YnjE was recently identified to act as a sulfur donor for Moco biosynthesis in *E. coli*. Because it was not clear whether *ynjE* is expressed as a single transcriptional unit or together with the *ydjXYZynjABCD* operon, we compared the expression of both *lacZ* fusions. The plasmid-born *lacZ* fusions were studied under aerobic and anaerobic conditions in BW25113, and β-galactosidase activities were determined as Miller units. As shown in Table 4, the *tusA-lacZ* transcriptional fusion showed no changes in response to the oxygen concentration, with a high expression level of about 11,000 Miller units. In comparison, the expression of genes coding for proteins involved in tRNA thiolation is 3-fold higher under anaerobic conditions in comparison with the aerobic conditions, as revealed by the *tusBCD-lacZ* promotor fusion. The results in Table 4 additionally show that *ynjE* is expressed mainly under anaerobic conditions (7.5-fold induction) and represents its own transcriptional unit. Although the *ydjXYZynjABCD-lacZ* fusion showed a generally low expression level, the expression was induced 10-fold under anaerobic conditions. However, the role of this operon remains unclear. The results show that the differences in expression of the genes identified by transcriptomic and proteomic analyses in response to the oxygen concentration are not based on differences in the expression of *tusA*, because the expression of *tusA* is not altered by the oxygen concentration in the cell. In contrast, the transcription of the *ynjE* gene, which is involved in Moco biosynthesis, is elevated under anaerobic conditions. This may imply that YnjE has a main role under anaerobiosis, which might be related to a higher expression of selected molybdoenzymes under these conditions.

*Analysis of the Activities of Hydrogenases, NR, and TMAOR in a Δ*tusA* Strain*—The microarray analysis showed that the gene expression of hydrogenase 3 and nitrate reductase in addition to their maturation factors are increased up to 4-fold in the Δ*tusA* mutant under anaerobic or aerobic conditions. We wanted to test whether the increased expression level correlates with an increase in enzyme activity. Thus, we tested the activity of hydrogenase, NR, and, as additional molybdoenzyme, TMAOR, in BW25113 cells and in the Δ*tusA* mutant after aerobic and anaerobic growth on nitrate or TMAO, respectively. For comparison regarding the effect of the absence of thiolated tRNA, we used the Δ*mnmA* strain as a control.

Hydrogenase activity was determined by detecting the reduced benzyl viologen-based hydrogen utilization. As shown in Table 5, the hydrogen oxidation was increased almost 4-fold in the Δ*tusA* strain, whereas it remained the same in the Δ*mnmA* strain in comparison with the wild type strain. The increase in activity is consistent with the 4-fold increased expression shown in Table 2.

Further, we analyzed the activity of TMAOR and NR. The respective *E. coli* strains were cultivated in the presence of 20 mM nitrate or 20 mM TMAO under aerobic conditions until the stationary phase was reached. NR activities and TMAOR activities in crude cell extracts were determined by analyzing the oxidation of benzyl viologen. As shown in Table 5, the activities of both NR and TMAOR were largely reduced down to 4–6% when purified from the Δ*tusA* strain in comparison with the wild type strain. In all cases, the effect on enzyme activity was not based on an altered level of thiolated tRNA, as the Δ*mnmA* strain showed enzyme activities comparable to BW25113. Thus, the absence of TusA influenced the activity of the two tested molybdoenzymes drastically.

TABLE 3

Detection of differently regulated proteins in *E. coli* JW3435 (Δ*tusA*) strain by two-dimensional gel electrophoresis

Strains BW25113 and Δ*tusA* were grown aerobically at 37 °C for 8 h. Two-dimensional gel electrophoresis was performed as described under "Experimental Procedures" and in the legend for Fig. 1. All proteins were identified by MALDI peptide mapping. Spot numbers refer to the numbering on the two-dimensional gel electrophoresis pictures (Fig. 1). Protein names, sizes, and functions are indicated. Protein scores greater than 70 are significant ($p < 0.05$). In total, five independent two-dimensional gel electrophoreses were performed. In respect to their increase/decrease of expression in Δ*tusA* in comparison with BW25113 wild type; the numbers indicate the quantity of identification in these five independent measurements.

Spot	Protein	Molecular mass	Score	Expression in Δ*tusA*	
				Higher	Lower
		kDa			
1	Molybdopterin synthase catalytic subunit, MoaE	17	156	5	
2	Chaperone protein, DnaK	69.2	221	5	
3	Flagellin, FliC	51.3	241	5	
4	Adenylate kinase, Adk	23.6	108	3	
5	Global transcriptional DNA-binding regulator, H-NS	15.6	115	2	
6	Stress response and acid-resistance protein, HdeA	12	97	2	1
7	Acid-resistance protein, HdeB	12.2	72	1	1
8	DNA protection during starvation protein, Fe-binding and storage protein Dps	18.7	145		1
9	DNA-binding transcriptional dual regulator of siderophore biosynthesis and transport, ferric uptake regulator, Fur	17	109		1
10	Outer membrane protein A, OmpA	37.3	173		2
11	Glucose-1-phosphatase, Agp	46	139		2
12	Methyl-galactoside transporter subunit, MglB	35.4	180		2
13	Ribosome-associated inhibitor A, RaiA	12.8	72		2
14	Maltose transporter subunit, MalE	43.4	175		3
15	Peroxiredoxin, OsmC	15.2	102		5
16	Periplasmic dipeptide transport protein, DppA	60.4	231		5

TABLE 4

β-Galactosidase activities of *lacZ* transcriptional fusions under aerobic and anaerobic growth conditions

BW25113 containing the *lacZ* transcriptional fusions were grown in LB until $A_{600\,nm}$ 0.6–1.0. β-Galactosidase activities were measured, and the Miller units were calculated as described under "Experimental Procedures." The average of at least three different measurements is shown.

lacZ-fusion	Aerobic	Anaerobic
tusA-lacZ	11,314 ± 835	10,608 ± 1,310
tusBCD-lacZ	2,991 ± 102	6,144 ± 752
ynjE-lacZ	417 ± 10	3,162 ± 17
ydjXYZynjABCD-lacZ	43 ± 4	421 ± 18

TABLE 5

Analysis of the activity of hydrogenase, *Ec*TMAOR, and *Ec*NR in the *E. coli* Δ*tusA* strain

Activites were measured as units/mg. For *E. coli* hydrogenases, specific enzyme activity is defined as 1 μmol of benzyl viologen reduced $min^{-1}mg^{-1}$. For *Ec*TMAOR and *Ec*NR, specific enzyme activity is defined as the oxidation of 1 μmol of benzyl viologen min^{-1} mg^{-1}.

Enzyme	BW25113	Δ*tusA*	Δ*mnmA*
	Units/mg	*Units/mg*	*Units/mg*
E. coli hydrogenases	6.56 ± 0.46	25.99 ± 2.25	9.12 ± 1.76
E. coli TMAOR	1.73 ± 0.04	0.07 ± 0.01	1.75 ± 0.05
E. coli NR	2.13 ± 0.05	0.13 ± 0.01	2.17 ± 0.06

Analysis of the Activities of Molybdoenzymes with Different Cofactor Modifications in the E. coli ΔtusA Strain—Molybdoenzymes with three different cofactor modifications were identified in *E. coli* belonging to the three classified families: DMSO reductase, sulfite oxidase, and xanthine dehydrogenase. To further characterize the effect of the *tusA* deletion on the molybdoenzymes of each family, we tested one characteristic enzyme from each family in regard to its activity in the Δ*tusA* strain. For this purpose we selected *E. coli* TMAOR containing bis-MGD, *E. coli* PaoABC containing MCD, *R. capsulatus* xanthine dehydrogenase (*Rc*XDH) containing sulfurated Mo-MPT, and human sulfite oxidase containing unmodified Mo-MPT. The respective molybdoenzymes were overexpressed in *E. coli* Δ*tusA* and BW25113 cells under aerobic conditions, purified by nickel-nitrilotriacetic acid chromatography, and analyzed for their MPT content and their saturation with molybdenum and iron (when appropriate). Consistent with the data shown above, all four molybdoenzymes (*Ec*PaoABC, human sulfite oxidase, *Rc*XDH, and *Ec*TMAOR) showed a loss of enzyme activity of 84.2–94% when purified from the Δ*tusA* strain (Table 6). Analysis of the metal content showed that whereas the purified enzymes were completely saturated with iron (except for *Ec*TMAOR, which contains Moco as sole cofactor), the molybdenum contents were down to a level of 3.7 to 15.3%, consistent with their enzyme activities (Table 6). Additionally, the MPT content (detected as form A) was reduced to 81.5–100% in a similar manner. Thus, the loss of enzyme activity correlated with a reduced Moco content in these enzymes, and the loss of activity was the same for molybdoenzymes from each family. This result shows that the effect of the absence of TusA has to be a general effect on Moco biosynthesis independent of further specific modifications of Moco.

Analysis of the Effect of Oxygen on the Activity of NR and TMAOR in Different E. coli Mutant Strains—The microarray analysis showed the effect of oxygen concentration on the expression of different genes in the Δ*tusA* mutant strain. As the results above showed that the activity of NR and TMAOR was largely reduced under aerobic conditions in the Δ*tusA* strain, we additionally wanted to test the activity under anaerobic conditions. To exclude an effect of tRNA thiolation on enzyme activity, we additionally tested NR and TMAOR activity in the Δ*tusD* and Δ*mnmA* strains. Additionally, two homologues of TusA were identified in *E. coli*, YeeD and YedF (14, 40), which share an amino acid sequence homology of 39% for YedF and 33% for YeeD. Thus far, YeeD and YedF had not been characterized and nothing is known about the role of these proteins in *E. coli*. To test whether YeeD or YedF could replace TusA in its role, at least partially, we additionally analyzed NR and

TABLE 6

Analysis of the activity and cofactor content of molybdoenzymes *Ec*TMAOR, *Ec*PaoABC, *Rc*XDH, and hSO in the *E. coli* Δ*tusA* strain in comparison with BW25113.

Molybdoenzyme produced	Activity[a]	MPT content[b]	Mo[c]	Fe[c]
	%	%	%	%
*Ec*TMAOR	6	0	3.7	0
*Ec*PaoABC	15.8	14.5	14.2	112
*Rc*XDH	8.7	9	12.7	104
*h*SO	13.5	18.5	15.3	105

[a] Specific enzyme activities were determined as units/mg, which are defined as 1 μmol of benzyl viologen oxidized min^{-1} mg^{-1} for *Ec*TMAOR, 1 μmol of vanillin oxidized $min^{-1}mg^{-1}$ for *Ec*PaoABC, 1 μmol of NADH produced $min^{-1}mg^{-1}$ for *Rc*XDH, and 1 μmol of sulfite oxidized $min^{-1}mg^{-1}$ for hSO. The activity of enzymes purified from BW25113 was set to 100%.

[b] MPT was quantified as relative form A fluorescence from the peak areas. The fluorescence detected in enzymes purified from in BW25113 was set to 100%.

[c] Molybdenum (μM molybdenum/μM enzyme) and iron (μM iron/μM enzyme) contents were determined by ICP-OES (see "Experimental Procedures"). The metal content of enzymes purified from BW25113 was set to 100%.

TMAOR activities in Δ*yeeD* and Δ*yedF* mutants in addition to a Δ*tusA*Δ*yedF*Δ*yeeD* triple mutant.

The strains were cultivated in the presence of either 20 mM nitrate or 20 mM TMAO under aerobic and anaerobic conditions, respectively. As shown in Fig. 2, the deletion of *tusD* or *mnmA* did not affect the activity of NR and TMAOR in comparison with the corresponding wild type strain under the different growth conditions. This shows that an impairment of 2-thiouridine formation does not affect molybdoenzyme activities. As described above, NR and TMAOR activity were decreased up to 96% in the Δ*tusA* strain under aerobic conditions. However, under anaerobic conditions, the effect of the Δ*tusA* mutant was less pronounced, showing a decrease in NR activity of 52% and of TMAOR activity of 74% in comparison with the wild type strain.

To determine whether the remaining activities of NR and TMAOR in the Δ*tusA* mutant strain were based on the partial replacement of TusA function by its two homologues, YeeD and YedF, we analyzed the enzyme activities in single, double, and triple mutant strains of these genes. The results in Fig. 2 show that neither YedF nor YeeD are able to replace TusA in its function, because single *yedF* and *yeeD* deletions did not affect molybdoenzyme activities and the triple Δ*tusA*Δ*yedF*Δ*yeeD* mutant showed the same effect on enzyme activity as the single Δ*tusA* strain. The results show conclusively that whereas TusA is almost essential for the activity of NR and TMAOR under aerobic conditions, the absence of TusA only partially affects molybdoenzyme activities under anaerobic conditions. Thus, under anaerobic conditions other proteins different from YedF or YeeD can take over the role of TusA for Moco biosynthesis.

Analysis of the Effect of TusA on the MPT and cPMP Content in Addition to the Sulfuration Level of MPT Synthase—The results above show that TusA has a major effect on Moco biosynthesis under aerobic conditions, which is independent of the modification of the cofactor. Because TusA is involved in sulfur transfer to tRNA, it might additionally be involved in sulfur transfer for the generation of the dithiolene moiety of Moco. So far, it has been shown that the direct donor for the sulfur in Moco is the MoaD protein, inserting sequentially the sulfur of its C-terminal thiocarboxylate group into cPMP, thus forming MPT (22). As a consequence, cPMP is accumulated in a *moaD* mutant. The direct sulfur donor for MoaD is the IscS protein, which generates the thiocarboxylate group on MoaD in conjunction with MoeB (25). YnjE is also involved in this step, making the sulfur transfer reaction from IscS more specific (5). To test whether TusA is additionally involved in the sulfur transfer reaction from IscS to MoaD, we analyzed the sulfuration level of MoaD isolated from a Δ*tusA* mutant. The sulfuration level of MoaD was analyzed by testing its ability to convert cPMP to MPT in conjunction with its partner protein, MoaE (forming active MPT synthase). MoaD, MoaE, and MoeB were expressed under aerobic conditions, purified from the BW25113(DE3), Δ*tusA*(DE3), and Δ*mnmA*(DE3) strains, and incubated with an excess amount of cPMP. The MPT produced was quantified by its conversion to the fluorescent derivate, form A. The activity of MPT synthase isolated from the wild type strain was set at 100%. As shown in Fig. 3*A*, MPT synthase purified from the Δ*tusA* strain showed a residual activity of 10% in comparison with the MPT synthase isolated from BW25113(DE3). The Δ*mnmA* strain did not affect MPT synthase activity, showing that this effect is independent of tRNA thiolation.

Because the results showed that MPT synthase activity is highly reduced in the Δ*tusA* mutant strain, we determined the total cPMP and MPT concentrations. Strains were grown aerobically and anaerobically in the presence of 20 mM nitrate. For comparison, a Δ*moaA* strain was chosen that does not contain cPMP or MPT.

In crude extracts of different mutant strains, cPMP and MPT were oxidized to their stable fluorescence derivatives, compound Z and form A, respectively (Fig. 3, *B* and *C*). The amount of cPMP determined in the Δ*moaD* strain was set individually to 100% under aerobic and anaerobic conditions (Fig. 3*B*). Although in the wild type, the Δ*mnmA* mutant, and the Δ*moaA* mutant, no cPMP was identified, the Δ*tusA* mutant accumulated 75% cPMP under aerobic conditions and 40% cPMP under anaerobic conditions when compared with the Δ*moaD* strain.

For the overall MPT levels determined in these strains, the MPT content of the wild type under the two growth conditions was set individually to 100% (Fig. 3*C*). Whereas the Δ*mnmA* strain showed comparable levels as the wild type strain, the MPT level in the Δ*tusA* strain was reduced to 80% under aerobic growth conditions and to 70% under anaerobic growth conditions. In comparison, no MPT was detected in the Δ*moaA* and Δ*moaD* strains.

The results are consistent with the activity of molybdoenzymes analyzed in the Δ*tusA* strain, showing that under aerobic conditions, less Moco is produced. Additionally, the results show that TusA has a role in sulfur transfer for the conversion of cPMP to MPT, because in a Δ*tusA* mutant, cPMP is accumulated. However, TusA is not essential in this reaction, because under anaerobic conditions the absence of TusA only leads to a reduction of about 50% of MPT.

Additionally, we analyzed the metal contents of the crude extract (Fig. 4*A*) and the membrane fraction (Fig. 4*B*) of these mutant strains. The results show that whereas the molybdenum content in the Δ*tusA* strain correlated well with the activity of NR in this strain, the concentration of other metals (iron, cop-

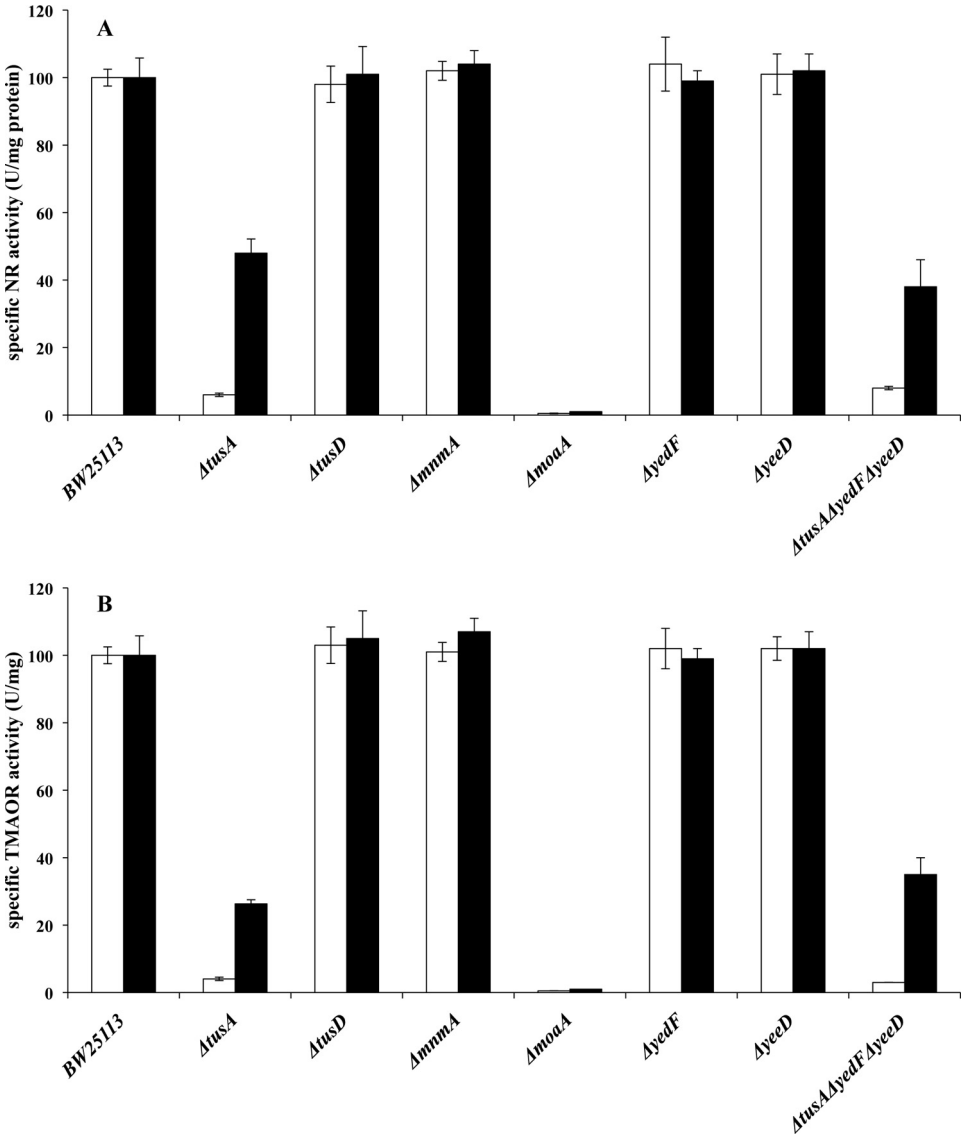

FIGURE 2. **Analysis of NR and TMAOR activity in different *E. coli* strains.** NR activity (*A*) and TMAOR activity (*B*) were determined by using cell lysates of the strains BW25113, JW3435 (Δ*tusA*), JW3305 (Δ*tusD*), JW1119 (Δ*mnmA*), JW1994 (Δ*yeeD*), JW1915 (Δ*yedF*), and JW3435/1994/1915 (Δ*tusA*Δ*yeeD*Δ*yedF*), which were grown aerobically (*white bars*) and anaerobically (*black bars*) in the presence of 20 mM nitrate and TMAO, respectively. Reduced benzyl viologen was used as an electron donor. The activity of the wild type strain under aerobic and anaerobic growth conditions was set to 100% each and compared with the mutant strains under the same growth conditions. The activities were related to total protein concentration in the crude extract. *Error bars* are derived from three independent measurements within a standard deviation of 10% at maximum.

per, or nickel) was not influenced by the absence of TusA. The decrease in molybdenum content in the membrane fraction is based on the reduced synthesis of membrane-bound molybdoenzymes like NR. The overall reduced molybdenum content shows a feedback regulation of impaired Moco biosynthesis and molybdate uptake (as revealed by the decreased expression of the *mod* operon in the Δ*tusA* strain).

Analysis of the Effect of Overexpression of the ISC Genes on Molybdoenzyme Activity—The above results show that TusA is involved in the sulfur transfer step for Moco biosynthesis. However, because TusA has a more pronounced effect under aerobic conditions than under anaerobic conditions, where the absence of TusA leads to only a 50% reduction of molybdoenzyme activities, we suspected that TusA might not be involved directly in Moco biosynthesis and that the effect is more general in the distribution of sulfur in the cell. Because the expression of a lot of genes for molybdoenzymes that are regulated by FNR was increased under anaerobic conditions in a Δ*tusA* strain, we suspected that the availability of TusA might influence the level of FeS clusters in the cell, as suggested previously by Maynard *et al.* (13). To analyze the effect of an increased level of FeS cluster biosynthesis on molybdoenzyme activity, we overexpressed the *A. vinelandii iscSUAhscABfdxiscX* operon in BW25113 under aerobic and anaerobic conditions. The activity of NR and TMAOR was determined and related to the activity determined in BW25113. The results in Fig. 5*A* show that NR activity was reduced to 10% under aerobic conditions and 41% under anaerobic conditions, whereas TMAOR activity was reduced to 30% under aerobic conditions and 53% under anaerobic conditions in comparison with the strain in which the ISC operon was not expressed. Thus, the reduced activities of NR and TMAOR in the presence of a higher level of FeS clusters in the cell are

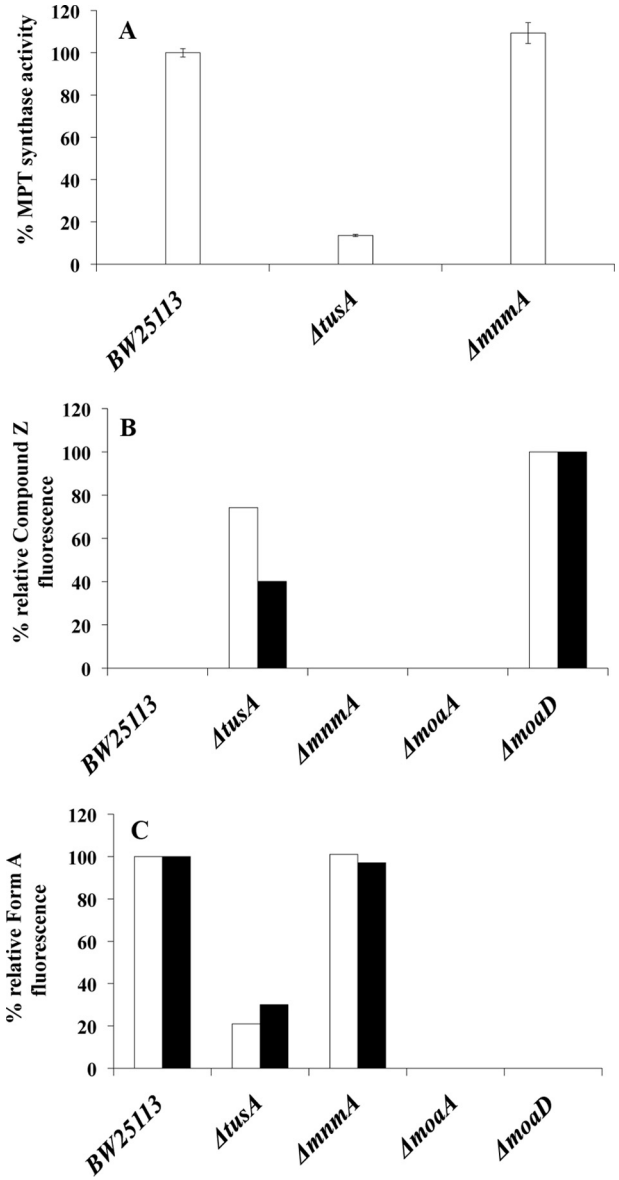

FIGURE 3. **Analysis of MPT synthase activity and cPMP and MPT concentrations in different *E. coli* strains.** *A*, MPT synthase was expressed in *E. coli* strains BW25113(DE3), JW3435 (Δ*tusA*)(DE3), and JW1119 (Δ*mnmA*)(DE3) and purified after ammonium precipitation and size exclusion chromatography. To analyze the sulfuration level of MPT synthase, 15 μM purified MPT synthase was incubated with an excess of cPMP. After 45 min, the reactions were stopped by the addition of acidic iodine, and MPT formed during the reaction was quantified as form A using the peak area. Fluorescence was monitored with excitation at 383 nm and emission at 450 nm. The activity of the wild type strain was set to 100%. Results were derived from at least three measurements, and standard deviations are within a range of 10%. *B*, quantification of cPMP concentration in *E. coli* strains JW3435 (Δ*tusA*), JW1119 (Δ*mnmA*), JW0764 (Δ*moaA*), and JW0767 (Δ*moaD*) after oxidation to its stable fluorescent derivative, compound Z. Fluorescence was monitored with excitation at 370 nm and emission at 450 nm. The amount of compound Z of the Δ*moaD* strain was set to 100%. The concentrations were related to cell density determined at $A_{600\ nm}$. *C*, total MPT content of strains JW3435 (Δ*tusA*), JW1119 (Δ*mnmA*), JW0764 (Δ*moaA*), and JW0767 (Δ*moaD*). MPT was quantified after conversion to its fluorescence derivative, form A, and is shown as relative form A fluorescence quantified from the peak areas. The fluorescence obtained from the wild type strain was set to 100%. Fluorescence was monitored with excitation at 383 nm and emission at 450 nm. *Black bars*, anaerobic growth conditions; *white bars*, aerobic growth conditions.

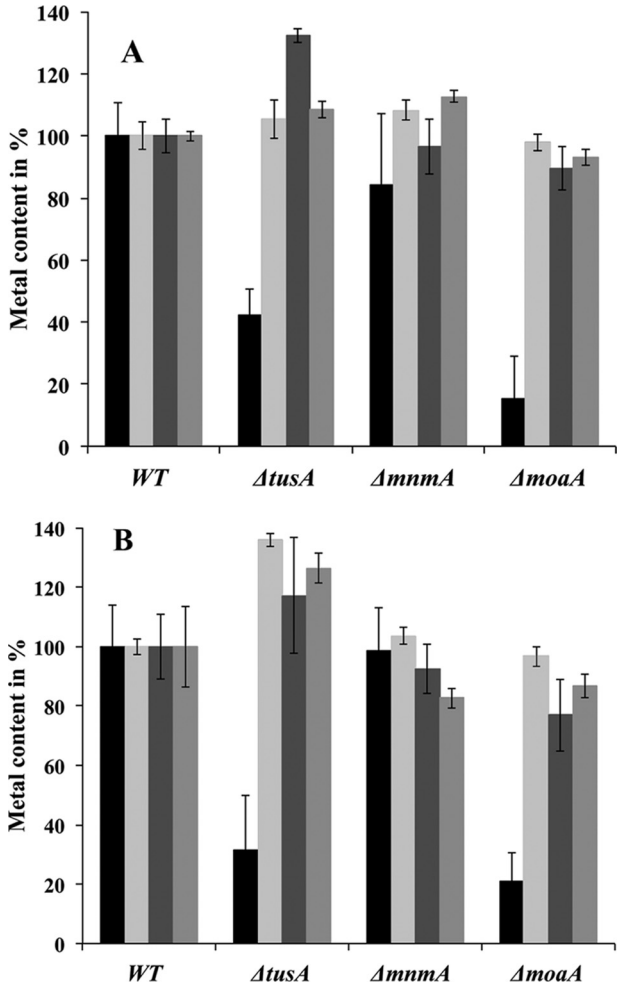

FIGURE 4. **Analysis of metal concentrations in different *E. coli* strains.** Total crude extracts and membrane fractions were prepared from *E. coli* strains BW25113, JW3435 (Δ*tusA*), JW1119 (Δ*mnmA*), and JW0764 (Δ*moaA*). ICP-OES was used to analyze levels of molybdenum (*black*), iron (*light gray bars*), nickel (*dark gray bars*), and copper (*gray bars*) in total crude extract (*A*) and in the membrane fraction of each strain (*B*). The metal content of the wild type strain was set to 100%. All metal contents were related to the total protein concentration. Results were derived from at least three independent measurements, and standard deviations are within a range of 20%.

consistent with the reduced activities of different molybdoenzymes when TusA is absent.

Further, the opposite should occur when TusA is overexpressed in the cell. Then, sulfur transfer from IscS is directed away from FeS cluster biosynthesis. To test this hypothesis, we overexpressed TusA and IscU for comparison in BW25113 cells. The results in Fig. 5*B* show that the effect of an overexpression of IscU on NR and TMAOR activity is similar to the expression of the whole *iscSUAhscABfdxiscX* operon. Expression of IscU resulted in a reduced NR and TMAOR activity of 25–39% in comparison with cells in which IscU was not expressed. Surprisingly, when TusA was overexpressed, the activity of NR and TMAOR was not increased (Fig. 5*B*). Both NR and TMAOR activities were decreased to a level of 25–32%, in a manner similar to the IscU mutant. Here, we suspect that again the FeS level has an effect on Moco biosynthesis for NR and TMAOR. Because MoaA contains two 4Fe4S clusters, the synthesis of cPMP is affected when TusA is overexpressed, as

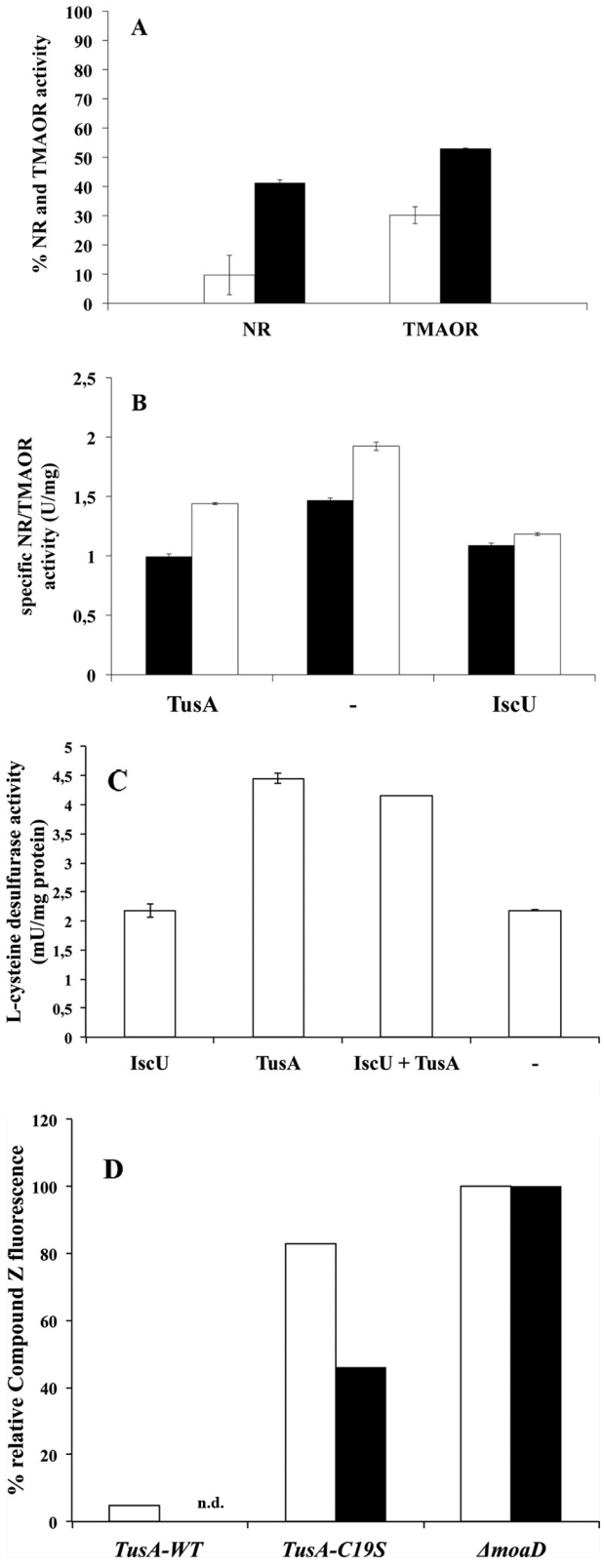

FIGURE 5. **Analysis of NR and TMAOR activities after overexpression of the ISC operon, TusA, and IscU.** *A*, plasmid encoding the *A. vinelandii* ISC operon was introduced into BW25113 (DE3), and the cells were grown for 8 h at 37 °C under aerobic (*white bars*) and anaerobic (*black bars*) conditions in the presence of either 20 mM nitrate or 20 mM TMAO, respectively. NR and TMAOR activities were determined in cell lysates. Reduced benzyl viologen was used as the electron donor. The activity of the wild type strain containing an arabinose-induced ampicillin-resistant plasmid was set to 100% for each condition. The activities were related to total protein concentration in the crude extract. *Error bars* are derived from three independent measurements within a standard deviation of 10% at maximum. *B*, plasmids encoding IscU (pJD54), TusA (pJD34), and pET15b (−) were introduced into BW25113 (DE3), and the cells were grown for 8 h at 37 °C in the presence of either 20 mM nitrate or 20 mM TMAO under aerobic conditions. TMAOR activities (*white bars*) and NR activities *(black bars*) were determined in cell lysates as described for Table 5. *C*, plasmids encoding IscU (pJD54), TusA (pJD35), and pACYCDuet (−) were introduced into BW25113 (DE3), and the cells were grown for 8 h at 37 °C under aerobic conditions. Cleared cell lysates were incubated with 500 μM L-cysteine for 10 min at 30 °C, and L-cysteine desulfurase activity was measured by determining total sulfide produced using methylene blue as reported previously (29). *D*, plasmids encoding TusA (pJD34), TusA-C19S (pJD49), and pET15b (−) were introduced into Δ*tusA*(DE3) and Δ*moaD,* respectively, and the cells were grown for 8 h at 37 °C in 20 mM nitrate containing LB under aerobic conditions with (*black bars*) and without (*white bars*) the addition of IPTG. Quantification of cPMP concentration was performed after oxidation to its stable fluorescent derivative, compound Z. Fluorescence was monitored with excitation at 370 nm and emission at 450 nm. The amount of compound Z of the Δ*moaD* strain was set to 100%. The concentrations were related to protein concentration in crude extract. *n.d.*, not determined.

fewer FeS clusters are available for the insertion into MoaA. Thus, overexpression of TusA directs IscS away from FeS cluster biosynthesis.

Analysis of the L-Cysteine Desulfurase Activity in Vivo—TusA was shown to enhance the L-cysteine desulfurase activity of IscS *in vitro*, whereas IscU has no such an effect on IscS, as reported recently (9, 41). IscS has different binding partners, namely IscU, CyaY, TusA, ThiI, and IscX (7). The binding sites for these proteins on IscS were mapped. Some proteins were shown to have overlapping binding sites. Thus, the binding of the different proteins to IscS might be regulated by their availability, suggesting that one protein outcompetes the other when available in higher concentrations. To test whether the direction of sulfur transfer from IscS to TusA is regulated by the concentration of TusA or IscU in the cell, we performed coexpression experiments *in vivo*. TusA, IscU, or both TusA and IscU were overexpressed in BW25113 cells, and the effect on L-cysteine desulfurase activity was analyzed in cell lysates after aerobic growth. The results in Fig. 5*C* show that the L-cysteine desulfurase activity increased 1.9-fold in the lysates where TusA was expressed. The expression of IscU did not affect the L-cysteine desulfurase. In contrast, the L-cysteine desulfurase activity containing both IscU and TusA showed a further enhancement (a factor of 2.1). This shows that in the presence of IscU, TusA is still able to bind to IscS, resulting in an increase in its activity.

Analysis of Protein-Protein Interactions by Surface Plasmon Resonance Measurements—To determine the dissociation constants of TusA and IscU for interaction with IscS, SPR measurements were employed for real-time detection of specific interactions using the purified proteins. TusA, IscS, and IscU were immobilized on the CM5 chip via amine coupling.

The results obtained by SPR measurement for the protein pairs listed in Table 7 showed the lowest K_D values for the interaction of immobilized TusA with IscS (K_D = 0.304 μM). IscS and immobilized IscU showed a K_D value of 0.574 μM, whereas no dissociation constant for the interaction of IscU with TusA was obtained. A comparable value was obtained for the interaction of immobilized IscS with TusA (K_D = 0.966 μM). The interaction between immobilized IscS and IscU (K_D of 14.6 μM) was lowered, showing that IscS was immobilized in a conformation that inhibited this interaction but not the interaction with TusA. In general, the results obtained from SPR

TABLE 7
SPR measurement of protein-protein interactions using IscS, TusA, and IscU

Immobilized protein[a]	RU[b]	Protein partner[c]	K_D[d]	chi²
			μM	
IscS	1118	BSA	ND[e]	
IscS	1118	TusA	0.966	1.41
IscS	1118	IscU	14.6	0.363
IscS	1118	IscS	0.995	7.3
IscU	1049	BSA	ND[e]	
IscU	1049	TusA	ND[e]	
IscU	1049	IscU	2.49	0.142
IscU	1049	IscS	0.574	6.14
TusA	538	BSA	ND[e]	
TusA	538	TusA	ND[e]	
TusA	538	IscU	ND[e]	
TusA	538	IscS	0.304	0.949

[a] Proteins were immobilized via amine coupling.
[b] RU, resonance units.
[c] Proteins were injected using the KINJECT protocol, injecting samples in a concentration range of 0.4 to 20 μM. Cells were regenerated by injection of 20 mM HCl.
[d] K_D values were obtained by global fitting procedures for a 1:1 binding.
[e] ND, no binding detectable (<1 RU).

show that TusA and IscU have dissociation constants similar to those of IscS, so that a direct competition in dependence on their cellular concentration is possible.

Transcriptional Analysis of Different lacZ Fusions in E. coli Δtusa and Δfnr Strains—From the results in the above studies, we suspected that the availability of IscS for certain pathways is regulated by its interaction partners. One way to test whether FeS levels are increased in the absence of TusA is the analysis of the activity of FNR. In its active form, FNR contains a 4Fe4S cluster, which enables FNR to bind to DNA and regulate the expression of genes. For this purpose, we analyzed the activity of FNR-regulated genes in different *E. coli* mutant strains. We constructed a *pepT-lacZ* fusion, which encodes peptidase T, as the expression of *pepT* has been shown to be activated by FNR (46). Additionally, we analyzed the expression of *ynjE* and *ydjXYZynjABCD*, genes that have been shown also to be regulated by FNR (46). Table 8 shows that the *pepT-lacZ* fusion has a 2–3-fold higher expression in the absence of *tusA,* implying a higher activity of FNR. Additionally, the expression of *ynjE* and *ydjxyZynjABCD* was enhanced 3-fold in a Δ*tusA* strain. In contrast, the expression of these genes/operons was decreased 2-fold in the Δ*fnr* strain. For comparison, we analyzed the expression of the *iscRSUA* operon in a *tusA*- and *fnr*-deficient strain. Although the expression of the operon was increased 13% in the Δ*tusA* strain, the expression was decreased 10% in the Δ*fnr* strain. Because the expression of the *iscRSUA* operon is regulated by the amount of FeS clusters in the cell via IscR, the result might be explained thus, that in the Δ*tusA* strain, FeS-containing molybdoenzymes are more highly expressed, simulating a higher demand for FeS clusters. In contrast, in the *fnr* mutant, the expression of genes for FeS-containing proteins is not activated, and thus the *iscRSUA* operon is down-regulated. In total, our transcriptional data imply a higher activity for FNR in the *tusA*-deficient strain, which would explain the different regulation of genes shown in our transcriptomic data (Table 2 and Supplemental Tables S1–S3).

Increased Amounts of TusA-C19S Lead to Decreased cPMP Accumulation in the Δtusa Mutant—To further dissect the influence of TusA on FeS cluster biosynthesis, we analyzed the influence of different expression levels of an inactive TusA variant on cPMP biosynthesis. For the synthesis of cPMP from GTP, the activity of the 4Fe4S cluster containing protein MoaA is required. Thus, a limited availability of FeS clusters should result in a decreased synthesis of cPMP due to the inactivity of MoaA.

To analyze the effects of TusA binding to IscS, we constructed the inactive TusA-C19S mutant and expressed the protein in the Δ*tusA* strain. TusA-C19S is still able to bind to IscS (data not shown); however, cPMP is accumulated under aerobic conditions because of the impairment in sulfur transfer for MPT biosynthesis. By the addition of IPTG, the expression of TusA-C19S was increased. Cells were grown under aerobic conditions, and the amount of cPMP was quantified and related to a Δ*moaD* mutant strain (set to 100%), which is completely impaired in the synthesis of MPT. As shown in Fig. 5*D*, the Δ*tusA* strain expressing TusA-C19S accumulated fewer amounts of cPMP in comparison with the Δ*moaD* strain. The amount of accumulated cPMP was decreased to 42% when IPTG was added. In comparison, the Δ*tusA* strain expressing TusA wild type did not accumulate cPMP, as sulfur is available for the synthesis of MPT. Thus, we propose that under the conditions tested, the higher amounts of expressed TusA-C19S compete with IscU for binding to IscS. Consequently, FeS cluster biosynthesis is decreased, resulting in a reduced level of active MoaA, which then results in the accumulation of cPMP.

DISCUSSION

The studies presented in this article show that TusA has a role in addition to tRNA thiolation in the cell. We suggest that TusA is involved in sulfur transfer for the synthesis of MPT and, in addition, is involved in the balanced regulation of the availability of IscS to various biomolecules in *E. coli*. In this report we studied the effects of a deletion of *tusA* in the cell in detail. Our studies show a pleiotropic effect of a Δ*tusA* mutant on the regulation of numerous genes in the cell (Table 2 and supplemental Tables S1–S3). Microarray analysis showed an increased expression of the *moaABCDE* operon in the absence of *tusA* independent of the growth conditions analyzed. Several molybdoenzymes, like NarGHI, NarZYV, XdhD, and FdhF, were found to be expressed up to 4-fold higher in the absence of *tusA* under anaerobic conditions or in the stationary phase. However, the determined activity of several molybdoenzymes from different families was largely decreased, up to 95%, under aerobic conditions. Further, we ascertained that cPMP is accumulated in the Δ*tusA* mutant and that this effect is stronger under aerobic conditions than in anaerobiosis. Because *tusA* is expressed in equal amounts under aerobic and anaerobic conditions, it could be excluded that this effect is based on different levels of TusA under various growth conditions. However, the results also showed that TusA is not essential for Moco biosynthesis, as 50% of the enzyme activities remained under anaerobic conditions. Because the expression of genes regulated by FNR (*hypABCDE*, *narGHJI*, *moaABCDE*, *soxS*, *cyoABCDE*, *sdhAB*, *tdcABCDEFG*, and *feoB*) was increased in the Δ*tusA* mutant, this let us to suspect that due to the absence of TusA, the level of IscS available for FeS cluster biosynthesis is increased. A higher level of FeS clusters in the cell might stabi-

TABLE 8

β-Galactosidase activities of *lacZ* transcriptional fusions expressed in different *E. coli* mutant strains

Strains containing the *lacZ* transcriptional fusions were grown anaerobically in LB containing 20 mM nitrate until $A_{600\ nm}$ 0.6–1.0. β-Galactosidase activities were measured, and the Miller units were calculated as described under "Experimental Procedures." The average of at least three different measurements is shown.

lacZ fusion	BW25113	Δ*tusA*	MC4100	Δ*fnr*
ydjXYZynjABCD-lacZ	422 ± 7	1,165 ± 170	105 ± 32	58 ± 6
ynjE-lacZ	3,021 ± 373	8,651 ± 619	963 ± 84	461 ± 110
iscRSUA-lacZ	3,071 ± 239	3,524 ± 144	6,400 ± 626	5,801 ± 392
pepT-lacZ	230 ± 9	452 ± 11	105 ± 10	64 ± 2

lize holoFNR, thus stimulating the transcription of FNR-regulated genes (like the genes for NR). However, a higher level of FeS clusters in the cell might also reduce the sulfur transfer of IscS to other biosynthetic pathways. To test this idea, we expressed the *A. vinelandii* ISC operon in *E. coli* cells. The results showed that an overexpression of the ISC operon has the same effect as IscU alone, or in the absence of TusA, on the activity of molybdoenzymes, decreasing their activity. Thus, a shift of the IscS pool in the cell has drastic effects on various pathways in the cell. Our conclusions are consistent with the results reported recently by Maynard *et al.* (13); these authors identify 2-thiouridine modification of $tRNA^{Lys}$ as responsible for the enhanced susceptibility of viral infection by inhibition of programmed ribosomal frameshifting. They show that the ISC FeS cluster biogenesis pathway exerts a protective effect and that a higher rate of binding of IscU to IscS is responsible for determining the rate of translational frameshifting (13). Here, computational modeling suggested a competitive binding of IscU and TusA to IscS (13). As a consequence of an increased FeS cluster pathway in the Δ*tusA* mutant, a protective effect during λ phage infection was observed, whereas an increased tRNA thiolation via TusA enhanced viral infection. Our results are consistent with their computational modeling results and the final model. Our results show that IscU and TusA have comparable dissociation constants with IscS; thus, they directly compete over binding to IscS. We suggest conclusively that one part of IscS in the cell is mostly in complex with IscU for FeS cluster biosynthesis and the other part may be available for other interaction partners such as TusA. Consistent with this hypothesis are studies by Marinoni *et al.* (42), who solved the crystal structure of the IscS-IscU complex from *Archaeoglobus fulgidus.* In the crystal structure the participation of the catalytic IscS-Cys321 as a transient ligand in the formation of the 2Fe2S cluster on IscU was resolved (42). Thus, during FeS cluster formation, a portion of IscS would not be available for acceptor proteins like TusA or ThiI. When the concentration of one of the interaction partner is changed (tested here for IscU and TusA), the IscS pool is shifted to one or the other direction, with a drastic effect on gene regulation.

With these findings, we propose a model (Fig. 6) that additionally tries to explain the differences in gene regulation observed in the micoarray data, which are very complex. We suggest that TusA is involved in sulfur transfer for the biosynthesis of Moco but, additionally, influences the FeS cluster biosynthesis in the cell.

Fig. 6*A* shows the situation of an *E. coli* wild type strain under anaerobic conditions. Here, the ISC operon is induced when FeS clusters are required, and IscS forms a complex with IscU for FeS cluster biogenesis. Among others, one regulator for the expression of genes under anaerobiosis is FNR, which contains an oxygen labile 4Fe4S cluster (43). FNR activates the transcription of the *moaABCDE* operon and the genes for nitrate reductase in *E. coli* (44). The *moaABCDE* operon codes for proteins involved in cPMP and MPT biosynthesis, with MoaA itself harboring two 4Fe4S clusters. The other IscS pool interacts with proteins like TusA, ThiI, CyaY, or IscX, for sulfur transfer to tRNA, thiamine, or MPT. Because TusA is not essential for the formation of MPT, its role might be replaced by other sulfur transfer proteins under anaerobic conditions. One sulfur carrier is the rhodanese-like protein YnjE, which is preferentially sulfurated by IscS (5). Additionally, our results showed that the expression of *ynjE* is increased under anaerobic conditions and in the absence of TusA, thus making it more available for sulfur transfer.

In the Δ*tusA* strain studied in this report, we propose that the pool of IscS is shifted, resulting in the misregulation of several pathways. Under aerobic conditions, generally fewer amounts of IscS are present, as the ISC operon is not induced (Fig. 6*B*). Also, FNR is mainly inactive, because the 4Fe4S cluster is converted to a 2Fe2S cluster, thereby inactivating FNR as a transcriptional regulator (45). In the absence of TusA, more IscS is available for the interaction with IscU, increasing the amount of FeS clusters in the cell. This results in an increased expression of the *moaABCDE* operon. Additionally, the amount of YnjE is decreased under aerobic conditions, and in the Δ*tusA* mutant the SUF system is less expressed. This leads to an impairment of the sulfur ability of all possible sulfur donors for MPT synthase required for the conversion of cPMP to MPT, thus resulting in an inactivity of almost all molybdoenzymes.

Under anaerobic conditions, the amount of IscS is generally increased. In the absence of TusA, the IscS pool is also shifted in the direction of IscU for FeS cluster biosynthesis (Fig. 6*C*). Increasing amounts of FeS clusters then switch FNR to its active state, inducing the transcription of genes like *soxS*, *moaABCDE*, *fdnGHI*, *dppA*, and *sodA* (44). Our studies showed that the genes for hydrogenase 3 were induced in the Δ*tusA* mutant, leading to 4-fold higher hydrogen utilization. Increased levels of FeS clusters into hydrogenase might result additionally in higher amounts of active enzyme.

The expression of different molybdoenzymes were differently affected in the Δ*tusA* mutant. Because the expression profile was recorded in strains grown on nitrate, the expression was additionally regulated by the activity of NarL. The availability of nitrate leads to activation of the transcriptional regulator NarL of many anaerobic electron transport- and fermentation-related genes (46, 47). The activity of NarL is dependent on the presence of nitrate, leading to its phosphorylation by NarX. NarL activates the expression of genes like *narGHI*, which are

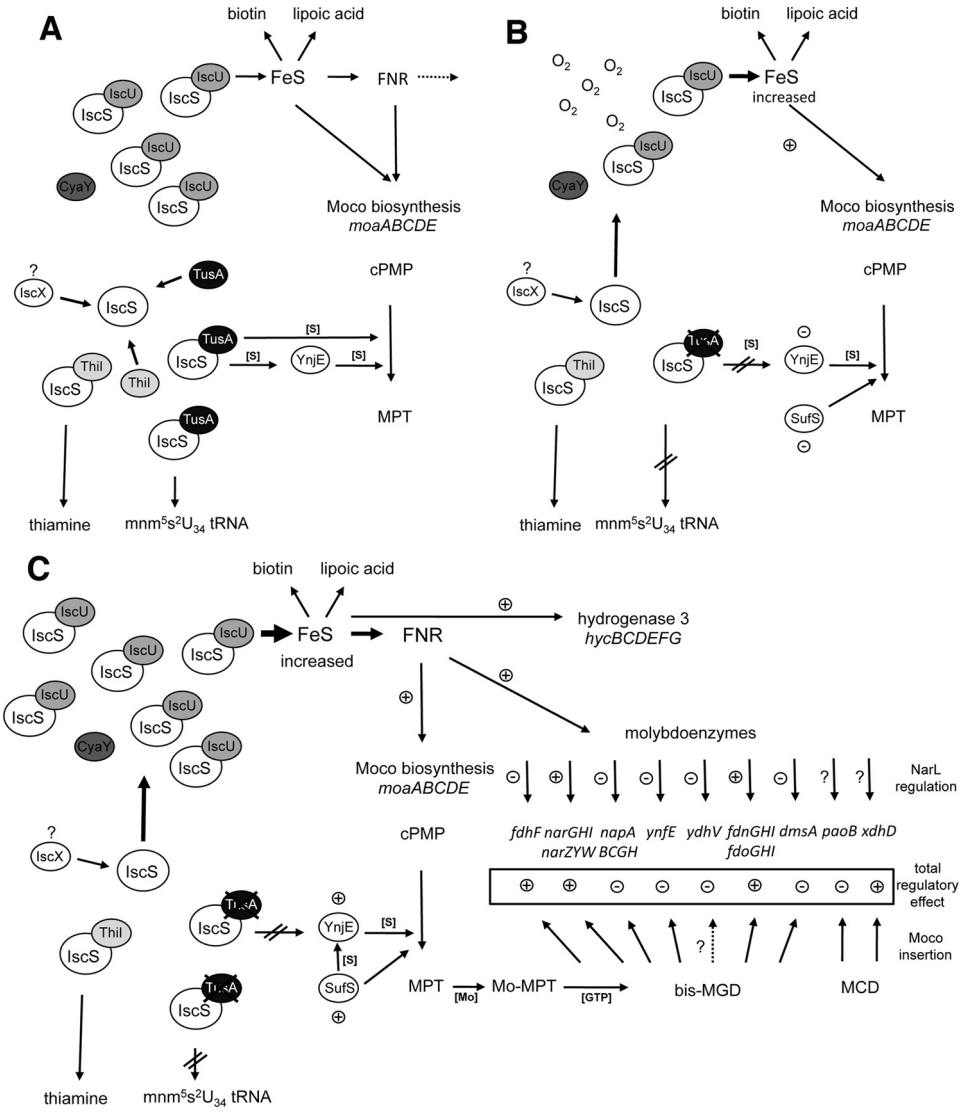

FIGURE 6. **Model for the role of TusA in *E. coli*.** *A*, the involvement of IscS in sulfur transfer under anaerobic conditions in *E. coli* wild type cells. *B*, sulfur transfer under aerobic conditions in the absence of TusA. *C*, sulfur transfer under anaerobic conditions in the absence of TusA. The model describes the data obtained from the microarray analysis with a focus of the effect on Moco biosynthesis and molybdoenzyme activities. A detailed description of the model is given in the text (under "Discussion").

required for nitrate respiration. These genes were also identified to be induced in the Δ*tusA* strain under aerobic conditions. Also identified as induced in the Δ*tusA* strain under anaerobic conditions (Fig. 6*C*). Additionally, NarL represses genes like *dmsA*, *ynfE*, and *ydhV*, which are involved in alternative respiratory pathways. The effect of the expression of molybdoenzymes taking together the regulation of FNR and NarL, which was determined by microarray analysis, is *boxed* in Fig. 6*C*.

Further, the activity of IscR might also be affected. IscR is negatively autoregulated and contains an FeS cluster that acts as a sensor of FeS cluster assembly (48). IscR activates the expression of the SUF system leading to increased expression of SufS under anaerobic conditions (49). In our microarray experiments, the expression of the SUF system was increased in the absence of *tusA* under anaerobic conditions, confirming this hypothesis. Additionally, under anaerobiosis the expression of *ynjE* is induced. Thus, the activity of various molybdoenzymes under anaerobic conditions in the Δ*tusA* strain was only reduced to a level of 50% (in the case of NR), as YnjE or SufS are available as sulfur donor for MPT biosynthesis and can replace IscS under these conditions. IscR usually shuts down the expression of the ISC operon when FeS clusters are present in sufficient amounts. However, we see an increased expression of the ISC operon in the Δ*tusA* mutant. This might be due to a higher expression of several molybdoenzymes, under these conditions, which also contain FeS clusters.

Conclusively, our studies show that the pleiotropic effect of a *tusA* deletion might be caused by changes in the FeS cluster concentration in the cell, leading to major differences in gene regulation. We propose that TusA is involved in regulating the IscS pool and shifting it away from IscU, thereby making IscS available for sulfur transfer for the biosynthesis of MPT. Whether TusA acts as a direct sulfur donor to provide the sulfur to MoeB/MoaD for Moco biosynthesis or other proteins like YnjE are involved as mediators in this reaction has to be investigated further in future studies.

Acknowledgments—We thank Lothar Lehnhardt and Zoya Ignatova (University of Potsdam) for their help with the two-dimensional gel electrophoresis experiments and Johannes Fritsch and Oliver Lenz (Humboldt University Berlin) for their support in the detection of hydrogenase activity. Nataliya Lupilova (Ruhr-University Bochum) and Angelika Lehmann (University of Potsdam) are thanked for their technical assistance. Roel M. Schaaper (NIEHS, National Institutes of Health) is thanked for the suggestion of initial experiments and helpful discussions. Mita Mullick Chowdhury and Julia Lücke (University of Potsdam) are thanked for initial experiments. We also thank Dennis Dean (Virginia Polytechnic Institute) for providing plasmid pDB1282 and Gottfried Unden (University of Mainz) for providing strain IMW151a.

REFERENCES

1. Kessler, D. (2006) Enzymatic activation of sulfur for incorporation into biomolecules in prokaryotes. *FEMS Microbiol. Rev.* **30,** 825–840
2. Mueller, E. G. (2006) Trafficking in persulfides: delivering sulfur in biosynthetic pathways. *Nat. Chem. Biol.* **2,** 185–194
3. Johnson, D. C., Dean, D. R., Smith, A. D., and Johnson, M. K. (2005) Structure, function, and formation of biological iron-sulfur clusters. *Annu. Rev. Biochem.* **74,** 247–281
4. Flint, D. H. (1996) *Escherichia coli* contains a protein that is homologous in function and N-terminal sequence to the protein encoded by the *nifS* gene of *Azotobacter vinelandii* and that can participate in the synthesis of the Fe-S cluster of dihydroxy-acid dehydratase. *J. Biol. Chem.* **271,** 16068–16074
5. Dahl, J. U., Urban, A., Bolte, A., Sriyabhaya, P., Donahue, J. L., Nimtz, M., Larson, T. J., and Leimkühler, S. (2011) The identification of a novel protein involved in molybdenum cofactor biosynthesis in *Escherichia coli*. *J. Biol. Chem.* **286,** 35801–35812
6. Hidese, R., Mihara, H., and Esaki, N. (2011) Bacterial cysteine desulfurases: versatile key players in biosynthetic pathways of sulfur-containing biofactors. *Appl. Microbiol. Biotechnol.* **91,** 47–61
7. Shi, R., Proteau, A., Villarroya, M., Moukadiri, I., Zhang, L., Trempe, J. F., Matte, A., Armengod, M. E., and Cygler, M. (2010) Structural basis for Fe-S cluster assembly and tRNA thiolation mediated by IscS protein-protein interactions. *PLoS Biol.* **8,** e1000354
8. Ayala-Castro, C., Saini, A., and Outten, F. W. (2008) Fe-S cluster assembly pathways in bacteria. *Microbiol. Mol. Biol. Rev*. **72,** 110–125
9. Ikeuchi, Y., Shigi, N., Kato, J., Nishimura, A., and Suzuki, T. (2006) Mechanistic insights into sulfur relay by multiple sulfur mediators involved in thiouridine biosynthesis at tRNA wobble positions. *Mol. Cell* **21,** 97–108
10. Ashraf, S. S., Sochacka, E., Cain, R., Guenther, R., Malkiewicz, A., and Agris, P. F. (1999) Single atom modification (O→S) of tRNA confers ribosome binding. *RNA* **5,** 188–194
11. Yokoyama, S., Watanabe, T., Murao, K., Ishikura, H., Yamaizumi, Z., Nishimura, S., and Miyazawa, T. (1985) Molecular mechanism of codon recognition by tRNA species with modified uridine in the first position of the anticodon. *Proc. Natl. Acad. Sci. U.S.A.* **82,** 4905–4909
12. Sylvers, L. A., Rogers, K. C., Shimizu, M., Ohtsuka, E., and Söll, D. (1993) A 2-thiouridine derivative in tRNAGlu is a positive determinant for aminoacylation by *Escherichia coli* glutamyl-tRNA synthetase. *Biochemistry* **32,** 3836–3841
13. Maynard, N. D., Macklin, D. N., Kirkegaard, K., and Covert, M. W. (2012) Competing pathways control host resistance to virus via tRNA modification and programmed ribosomal frameshifting. *Mol. Syst. Biol.* **8,** 567
14. Yamashino, T., Isomura, M., Ueguchi, C., and Mizuno, T. (1998) The *yhhP* gene encoding a small ubiquitous protein is fundamental for normal cell growth of *Escherichia coli*. *J. Bacteriol.* **180,** 2257–2261
15. Ishii, Y., Yamada, H., Yamashino, T., Ohashi, K., Katoh, E., Shindo, H., Yamazaki, T., and Mizuno, T. (2000) Deletion of the *yhhP* gene results in filamentous cell morphology in *Escherichia coli*. *Biosci. Biotechnol. Biochem.* **64,** 799–807
16. Leimkühler, S., Wuebbens, M. M., and Rajagopalan, K. V. (2011) The history of the discovery of the molybdenum cofactor and novel aspects of its biosynthesis in bacteria. *Coord. Chem. Rev.* **255,** 1129–1144
17. Neumann, M., Mittelstädt, G., Seduk, F., Iobbi-Nivol, C., and *Leimkühler*, S. (2009) MocA is a specific cytidylyltransferase involved in molybdopterin cytosine dinucleotide biosynthesis in *Escherichia coli*. *J. Biol. Chem.* **284,** 21891–21898
18. Rajagopalan, K. V. (1996) Biosynthesis of the molybdenum cofactor, in *Escherichia coli and Salmonella*. *Cellular and Molecular Biology* (Neidhardt, F. C., ed) pp. 674–679, ASM Press, Washington, D. C.
19. Hilton, J. C., and Rajagopalan, K. V. (1996) Identification of the molybdenum cofactor of dimethyl sulfoxide reductase from *Rhodobacter sphaeroides* f. sp. *denitrificans* as bis(molybdopterin guanine dinucleotide)molybdenum. *Arch. Biochem. Biophys.* **325,** 139–143
20. Pitterle, D. M., Johnson, J. L., and Rajagopalan, K. V. (1993) *In vitro* synthesis of molybdopterin from precursor Z using purified converting factor. Role of protein-bound sulfur in formation of the dithiolene. *J. Biol. Chem.* **268,** 13506–13509
21. Pitterle, D. M., and Rajagopalan, K. V. (1989) Two proteins encoded at the *chlA* locus constitute the converting factor of *Escherichia coli chlA1*. *J. Bacteriol.* **171,** 3373–3378
22. Gutzke, G., Fischer, B., Mendel, R. R., and Schwarz, G. (2001) Thiocarboxylation of molybdopterin synthase provides evidence for the mechanism of dithiolene formation in metal-binding pterins. *J. Biol. Chem.* **276,** 36268–36274
23. Rudolph, M. J., Wuebbens, M. M., Rajagopalan, K. V., and Schindelin, H. (2001) Crystal structure of molybdopterin synthase and its evolutionary relationship to ubiquitin activation. *Nat. Struct. Biol.* **8,** 42–46
24. Leimkühler, S., Wuebbens, M. M., and Rajagopalan, K. V. (2001) Characterization of *Escherichia coli* MoeB and its involvement in the activation of molybdopterin synthase for the biosynthesis of the molybdenum cofactor. *J. Biol. Chem.* **276,** 34695–34701
25. Zhang, W., Urban, A., Mihara, H., Leimkühler, S., Kurihara, T., and Esaki, N. (2010) IscS functions as a primary sulfur-donating enzyme by interacting specifically with MoeB and MoaD in the biosynthesis of molybdopterin in *Escherichia coli*. *J. Biol. Chem.* **285,** 2302–2308
26. Baba, T,, Ara, T., Hasegawa, M., Takai, Y., Okumura, Y., Baba, M., Datsenko, K. A., Tomita, M., Wanner, B. L., and Mori, H. (2006) Construction of *Escherichia coli* K-12 in-frame, single-gene knockout mutants: the Keio collection. *Mol. Syst. Biol.* **2,** 2006.0008
27. Schmitz, J., Wuebbens, M. M., Rajagopalan, K. V., and Leimkühler, S. (2007) Role of the C-terminal Gly-Gly motif of *Escherichia coli* MoaD, a molybdenum cofactor biosynthesis protein with a ubiquitin fold. *Biochemistry* **46,** 909–916
28. Ballantine, S. P., and Boxer, D. H. (1985) Nickel-containing hydrogenase isoenzymes from anaerobically grown *Escherichia coli* K-12. *J. Bacteriol.* **163,** 454–459
29. Urbina, H. D., Silberg, J. J., Hoff, K. G., and Vickery, L. E. (2001) Transfer of sulfur from IscS to IscU during Fe/S cluster assembly. *J. Biol. Chem.* **276,** 44521–44526
30. Wuebbens, M. M., and Rajagopalan, K. V. (1995) Investigation of the early steps of molybdopterin biosynthesis in *Escherichia coli* through the use of *in vivo* labeling studies. *J. Biol. Chem.* **270,** 1082–1087
31. Johnson, J. L., Hainline, B. E., Rajagopalan, K. V., and Arison, B. H. (1984) The pterin component of the molybdenum cofactor. Structural characterization of two fluorescent derivatives. *J. Biol. Chem.* **259,** 5414–5422
32. Genest, O., Seduk, F., Théraulaz, L., Méjean, V., and Iobbi-Nivol, C. (2006) Chaperone protection of immature molybdoenzyme during molybdenum cofactor limitation. *FEMS Microbiol. Lett.* **265,** 51–55
33. Neumann, M., Mittelstädt, G., Iobbi-Nivol, C., Saggu, M., Lendzian, F., Hildebrandt, P., and Leimkühler, S. (2009) A periplasmic aldehyde oxidoreductase represents the first molybdopterin cytosine dinucleotide cofactor containing molybdo-flavoenzyme from *Escherichia coli*. *FEBS J.* **276,** 2762–2774
34. Temple, C. A., Graf, T. N., and Rajagopalan, K. V. (2000) Optimization of expression of human sulfite oxidase and its molybdenum domain. *Arch. Biochem. Biophys.* **383,** 281–287
35. Truglio, J. J., Theis, K., Leimkühler, S., Rappa, R., Rajagopalan, K. V., and Kisker, C. (2002) Crystal structures of the active and alloxanthine-inhib-

ited forms of xanthine dehydrogenase from *Rhodobacter capsulatus*. *Structure* **10,** 115–125
36. Dietzel, U., Kuper, J., Doebbler, J. A., Schulte, A., Truglio, J. J., Leimkühler, S., and Kisker, C. (2009) Mechanism of substrate and Inhibitor binding of *Rhodobacter capsulatus* xanthine dehydrogenase. *J. Biol. Chem.* **284,** 8768–8776
37. Garrett, R. M., and Rajagopalan, K. V. (1996) Site-directed mutagenesis of recombinant sulfite oxidase. Identification of cysteine 207 as a ligand of molybdenum. *J. Biol. Chem.* **271,** 7387–7391
38. Iobbi-Nivol, C., Pommier, J., Simala-Grant, J., Méjean, V., and Giordano, G. (1996) High substrate specificity and induction characteristics of trimethylamine-*N*-oxide reductase of *Escherichia coli*. *Biochim. Biophys. Acta* **1294,** 77–82
39. Neumann, M., Stöcklein, W., Walburger, A., Magalon, A., and Leimkühler, S. (2007) Identification of a *Rhodobacter capsulatus* L-cysteine desulfurase that sulfurates the molybdenum cofactor when bound to XdhC and before its insertion into xanthine dehydrogenase. *Biochemistry* **46,** 9586–9595
40. Katoh, E., Hatta, T., Shindo, H., Ishii, Y., Yamada, H., Mizuno, T., and Yamazaki, T. (2000) High precision NMR structure of YhhP, a novel *Escherichia coli* protein implicated in cell division. *J. Mol. Biol.* **304,** 219–229
41. Iannuzzi, C., Adinolfi, S., Howes, B. D., Garcia-Serres, R., Clémancey, M., Latour, J. M., Smulevich, G., and Pastore, A. (2011) The role of CyaY in iron sulfur cluster assembly on the *E. coli* IscU scaffold protein. *PLoS One* **6,** e21992
42. Marinoni, E. N., de Oliveira, J. S., Nicolet, Y., Raulfs, E. C., Amara, P., Dean, D. R., and Fontecilla-Camps, J. C. (2012) (IscS-IscU)2 complex structures provide insights into Fe2S2 biogenesis and transfer. *Angew. Chem. Int. Ed. Engl.* **51,** 5439–5442
43. Moore, L. J., and Kiley, P. J. (2001) Characterization of the dimerization domain in the FNR transcription factor. *J. Biol. Chem.* **276,** 45744–45750
44. Kang, Y., Weber, K. D., Qiu, Y., Kiley, P. J., and Blattner, F. R. (2005) Genome-wide expression analysis indicates that FNR of *Escherichia coli* K-12 regulates a large number of genes of unknown function. *J. Bacteriol.* **187,** 1135–1160
45. Reinhart, F., Achebach, S., Koch, T., and Unden, G. (2008) Reduced apofumarate nitrate reductase regulator (apoFNR) as the major form of FNR in aerobically growing *Escherichia coli*. *J. Bacteriol.* **190,** 879–886
46. Constantinidou, C., Hobman, J. L., Griffiths, L., Patel, M. D., Penn, C. W., Cole, J. A., and Overton, T. W. (2006) A reassessment of the FNR regulon and transcriptomic analysis of the effects of nitrate, nitrite, NarXL, and NarQP as *Escherichia coli* K12 adapts from aerobic to anaerobic growth. *J. Biol. Chem.* **281,** 4802–4815
47. Unden, G., and Bongaerts, J. (1997) Alternative respiratory pathways of *Escherichia coli*: energetics and transcriptional regulation in response to electron acceptors. *Biochim. Biophys. Acta* **1320,** 217–234
48. Py, B., and Barras, F. (2010) Building Fe-S proteins: bacterial strategies. *Nat. Rev. Microbiol.* **8,** 436–446
49. Giel, J. L., Rodionov, D., Liu, M., Blattner, F. R., and Kiley, P. J. (2006) IscR-dependent gene expression links iron-sulphur cluster assembly to the control of O_2-regulated genes in *Escherichia coli*. *Mol. Microbiol.* **60,** 1058–1075
50. Eraso, J. M., and Weinstock, G. M. (1992) Anaerobic control of colicin E1 production. *J. Bacteriol.* **174,** 5101–5109
51. Dos Santos, P. C., Johnson, D. C., Ragle, B. E., Unciuleac, M. C., and Dean, D. R. (2007) Controlled expression of nif and isc iron-sulfur protein maturation components reveals target specificity and limited functional replacement between the two systems. *J. Bacteriol.* **189,** 2854–2862
52. Fürste, J. P., Pansegrau, W., Frank, R., Blöcker, H., Scholz, P., Bagdasarian, M., and Lanka, E. (1986) Molecular cloning of the plasmid RP4 primase region in a multi-host-range tacP expression vector. *Gene* **48,** 119–131
53. Casadaban, M. J. (1976) Transposition and fusion of the *lac* genes to selected promoters in *Escherichia coli* using bacteriophage λ and μ. *J. Mol. Biol.* **104,** 541–555
54. Unden, G., Becker, S., Bongaerts, J., Holighaus, G., Schirawski, J., and Six, S. (1995) O_2-sensing and O_2-dependent gene regulation in facultatively anaerobic bacteria. *Arch. Microbiol.* **164,** 81–90